Joint Optimization of Radar and Communications Performance in 6G Cellular Systems

Mateen Ashraf, Bo Tan, Dmitri Moltchanov, John S. Thompson, *Fellow, IEEE,* and Mikko Valkama, *Fellow, IEEE*

***Abstract*—Dual functional radar communication (DFRC) is a promising approach that provides a viable solution for the problem of spectrum sharing between communication and radar applications. This paper studies a DFRC system with multiple communication users (CUs) and a radar target. The goal is to devise beamforming vectors at the DFRC transmitter in such a way that the radar received signal-to-clutter-plus-noise-ratio (SCNR) is maximized while satisfying the minimum data rate requirements of the individual CUs. With regard to clutter, we consider two scenarios based on the possibility of clutter removal. Even though the formulated optimization problems are non-convex, we present efficient algorithms to solve them using convex optimization techniques. Specifically, we use duality theory and Karush-Kuhn-Tucker conditions to show the underlying structure of optimal transmit precoders. In the proposed solution, it is observed that there is no need to transmit separate probing signal for the radar detection in both the considered scenarios. This results in reduction in the number of optimization variables in the problem. Moreover, we make use of the asymptotic equivalence between Toeplitz matrices and Circulant matrices to further reduce the complexity of the proposed algorithm. Finally, numerical results are presented to demonstrate the effectiveness of the proposed algorithms.**

***Index Terms*—Detection probability, dual functional radar communication, integrated sensing and communication, resource allocation.**

I. Introduction

With the wide roll-out of commercial fifth generation (5G) mobile systems, the research communities have shifted the focus to identifying the enabling technologies and defining the key features of the sixth generation (6G). Unlike the previous generations, the 6G will penetrate all sectors and become a pervasive infrastructure resulting in massive network and end-user devices deployment. Consequently, the number of connected mobile devices is predicted to grow from 8B to 11.6B. Ericsson estimates the total mobile data traffic to reach around 65Exabytes (EB) per month, which is projected to grow by a factor of around 4.4 and reach 288EB per month by 2027 [1]. The wireless ICT systsems are estimated to cause about 4% of all electricity consumption and 2% of the CO2 emissions globally [2]. In the worst-case scenario, up to 51% of the global energy consumption could be due to ICT by 2030 [3] (the expected time for the launch of commercial 6G systems). Thus, energy efficiency (EE) becomes intrinsic requirement of 6G. Achieving high EE in radio networks requires the synergy of diverse techniques, including energy-efficient radio frequency (RF) components and circuits, novel signal processing and waveform designs, and optimized device and network operations. The first category includes several improvements in the components or hardware design like doherty power amplifier [4], high-isolation balun [5], epsilon negative-transmission line based antenna [6]. The second category incorporates efficient signal processing techniques like digital protestation [7], crest factor reduction [8], and hybrid beamforming [9].

Beside forecited approaches, cooperation based on mutual context-awareness among the network and user equipments (UEs) will help both sides optimize the transceiving schemes to save energy. In this scenario, new techniques that capture and model the location, motion status and environmental context, have become an emerging topic. Examples of such techniques include mobile computing, sensing, localization etc. In the same vein, recent research efforts are exploring the possibilities of joining wireless communications with radar systems. These efforts have led to a fascinating research field which is now known as integrated sensing and communication (ISAC) [10], [11]. In legacy mobile communication systems, the sensing functionality has been primarily achieved by using auxiliary information, for example, the global navigation satellite system (GNSS) or inertial sensor on devices. In 5G systems, various reference signals [12] are defined in uplink and downlink radio frames, which can be used for estimating the angle and distance of the transmitter [13] and even used for imaging [14] purpose. Moreover, 6G wireless networks aim to provide sensing as a service [15], where the quality of service (QoS) and EE are anticipated to be drastically improved compared to traditional systems. Therefore, conventional mechanisms to obtain sensing information may not meet expected performances. Specifically, the anticipated 6G wireless networks are required to support various emerging applications with low energy consumption, such as connected autonomous vehicles (CAV), connected everyday devices, drone monitoring and smart manufacturing, etc. The natural embedding of the sensing function in the mobile system is of utmost importance in these applications.

The sensing information can play a pivotal role in the communication systems, for example, to improve EE. With location information of the UE, the access point can direct beam toward the UE to improve the data rate for a fixed

M. Ashraf, B. Tan, D. Moltchanov and M. Valkama are with Faculty of Information Technology and Communication Sciences, Tampere University, Finland. (e-mails: {mateen.ashraf, bo.tan, dmitri.moltchanov, mikko.valkama}@tuni.fi).

John S. Thompson is with Institute for Digital Communications, School of Engineering, The University of Edinburgh, United Kingdom, EH9 3BF. (e-email: john.thompson@ed.ac.uk).

This work was in part supported by the Academy of Finland ACCESS project (Autonomous Communication Converged with Efficient Sensing for UAV Swarms, Project No. 339519) and 5G-PSS (5G Positioning, Sensing and Security Functions) through Business Finland under Grant 6868/31/2021.

emitting power or reduce energy consumption for a fixed data rate requirement. Hence, it is expected that the communication performance will be greatly improved if UEs can be detected, localized and tracked [15]. Therefore, dual functional radar communication (DFRC) systems have been envisaged to deal with the feasibility of using the same access point for transmitting information to communication users (CUs) and detecting radar targets, resulting in integration gain and coordination gain [15]. This paper studies a DFRC system and optimizes the detection performance of the radar target while simultaneously satisfying the essential communication performance requirements.

Similarly to 5G systems, where low ($<$ 1 GHz), mid ($1 \sim 6$ GHz, so-called, sub-6 GHz band) and high ($>$ 20 GHz, millimeter wave (mmWave) band) frequency bands are defined [16], 6G will likely utilize multiple bands for communications [17]. Based on the recent research in [18]–[20], the higher frequency signals have more pronounced benefits on sensing resolution, EE via frequency, waveform and waveform sharing mechanisms becasue of the ample specturm resorces.However, in this paper, we still focus on exploiting legacy sub-6 GHz band that is available for 5G system and will likely be available in 6G as well. The rationale is that although mmWave or terahertz (THz) frequency bands in 5G/6G will utilize much wider bandwidth, their propagation properties are greatly affected by attenuation and blockage from static objects [21], [22] such as buildings and dynamic objects such as humans, vehicles, etc [23], [24]. To avoid these impacts, we concentrate on sub-6 GHz band, that is characterized by smaller bandwidth but blockage impairments are limited to $2 \sim 4$ dB [21] in our study.

This paper considers a DFRC with multiple CUs and a radar target. The aim is to maximize the radar detection probability whilst satisfying the minimum data rate requirements of CUs. We consider the following two scenarios with regard to the treatment of clutter in the environment.

- *First scenario*: We assume that the radar has the capability to suppress all reflections received from environmental clutter. In the case of imperfect cancellation, this scenario also deals with the possibility where the residual interference caused by the clutter at the radar receiver can be modeled as a zero-mean complex wide-sense stationary Gaussian process [25].
- *Second scenario:* We assume that no suppression is used for reflections received from the clutter. Hence, it may not be possible to approximate the interference caused by the clutter with a zero-mean complex wide-sense stationary Gaussian process.

The sensing function is performed via beamforming as the previous literature [26]. Different from the estimation based performance evaluation metrics in [27], we adopt the detection rate as performance metrics in this work. The maximization of the radar detection is achieved by properly designing transmit beamforming vectors. Specifically, it is observed that in both considered scenarios there is no need to transmit a separate probing signal for target. This observation reduces the complexity of the optimization algorithm and the feedback requirements of the system. Otherwise, the information related to probing signal would be required at the CUs to perform interference cancellation. In summary, the main contributions of the paper are listed as follows:

- We provide the globally optimal solution for the problem of detection probability maximization in ISAC systems with perfect clutter suppression. Specifically, closed-form expressions for optimal transmit beamforming vectors for individual CUs are provided. These expressions provide an insight on the solution structure for optimal beamforming.
- Then, the system model is extended to the scenario without clutter suppression. We solve the detection probability maximization problem through an iterative algorithm and for each iteration, we provide closed-form expressions for the globally optimal transmit beamformors.
- For both scenarios, there is no need to transmit a dedicated precoding signal for target detection. This observation has two implications. First, it reduces computational complexity of the algorithm by reducing the number of optimization variables. Secondly, this observation leads to reduced overhead exchange which may be required otherwise to cancel the interference caused by the dedicated probing signal. Moreover, in order to further reduce the complexity in each iteration for the second scenario, we propose a low complexity algorithm which utilizes an important property of the reflected signal from the clutter.

Our motivation is to reduce algorithm complexity when large number of optimization variables are involved in the optimization problems due to high number of antennas and downlink CUs. Moreover, the desire for having low-complexity algorithms in ISAC system is compounded by the fact that in a practical system target detection may be performed in various directions successively due to the absence of apriori information about the target direction and the motion of the target. Therefore, it is highly desirable to obtain the optimal beamforming solutions for any specific direction with least possible delay. To achieve this objective, in this paper we use the convex optimization theory to obtain closed-form solutions for the optimal transmit beamforming vectors. Hence, the proposed approach has considerably less computational complexity. Additionally, the availability of the closed-form solutions provides the optimal solution structures which are highlighted through remarks in Section IV.

The rest of this paper is organized as follows. Section II provides a literature review of related works. Section III discusses the system model and assumptions. The optimization framework and proposed algorithms are provided in Section IV. Section V presents a low complexity algorithm for solving the optimization problem in second scenario, where clutter cannot be suppressed. Numerical results are presented in Section VI. Finally, the paper is concluded in Section VII.

Notations: The notations used in this paper are given as follows. The sets of complex, real numbers are represented by $\mathbb{C}, \mathbb{R}$, respectively. Vectors and matrices are represented by bold small and capital letters, respectively. $\mathbf{A}^H, \mathbf{A}^{-1}, \mathrm{Tr}(\mathbf{A}), \mathrm{rank}(\mathbf{A})$ are the hermitian transpose, in-

verse, trace, rank and Frobenius norms of the complex matrix $\mathbf{A}$, respectively. $\mathbf{A} \succeq \mathbf{0}$ means that $\mathbf{A}$ is positive semidefinite. The magnitude of a scalar a and a vector $\mathbf{x}$ are represented by $|a|, \|\mathbf{x}\|$, respectively. $E(x)$ denotes the expectation of random variable x.

II. Related Work and Motivation

When embedding the sensing functions in the communications system, the performance metrics of ISAC are different from conventional communication systems. The commonly used performance metrics in ISAC system are Crámer-Rao bounds (CRBs) for sensing parameters estimations and the probability of detection. Specifically, for localization purposes, the goal is to devise the transceiving schemes approach to CRB. The goal of detection is to allocate transmission resources in such a way that the detection probability is maximized.

In terms of localization performance, recent works [28]–[32] provided CRB minimization schemes under different system setups. In [28], a hybrid approach with known/unknown placements of multiple sensors is presented to estimate locations of multiple targets. Various detectors based on the minimization of the CRB are presented in [29]. The works in [28], [29] do not consider the joint operation of sensing and communication. In terms of ISAC, a CRB minimization scheme is proposed in [30]. Specifically, the CRB is used as a performance metric for target angle estimation, and then a CRB minimization beamforming design is proposed which guarantees a predefined level of signal-to-interference-plus-noise ratio (SINR) for each CU. This work is further extended in [31] to design an energy efficient ISAC system with the help of antenna selection. In particular, the l_0 norm is used to select the number of active antennas to reduce the energy consumption at the DFRC. [32] investigated an over-the-air computation aided DFRC with a beamforming scheme to encompass different performance aspects of the integrated sensing, communication and computation system.

For detection probability maximization, it is well known that detection probability is an increasing function of the radar received signal-to-clutter-plus-noise ratio (SCNR) [33]. Much effort is devoted to guarantee the constant modulus and similarity properties of radar waveforms which include sequential optimization algorithms (SOAs) [34], the successive quadratically constrained quadratic programming (QCQP) [35], the block coordinate descent (BCD) framework [36], and the general majorization minimization (MM) framework [37]. In works [33]–[37], authors make assumption on the *a priori* information of the target, which is difficult to obtain in practice. Hence, an efficient beamforming design is proposed in [38] where no such assumption is made. It is concluded in [38] that using dedicated probing signal can improve the detection performance of the radar in presence of clutters when interference cancellation for radar signal is applied at CUs. To reap the benefits of orthogonal frequency division multiple (OFDM) access in ISAC systems, a joint OFDM waveform design is proposed in [39] to increase the reflected signal power under interference and auto-correlation constraints. In order to reduce the complexity of this work, a low complexity design is proposed in [25] for a single CU.

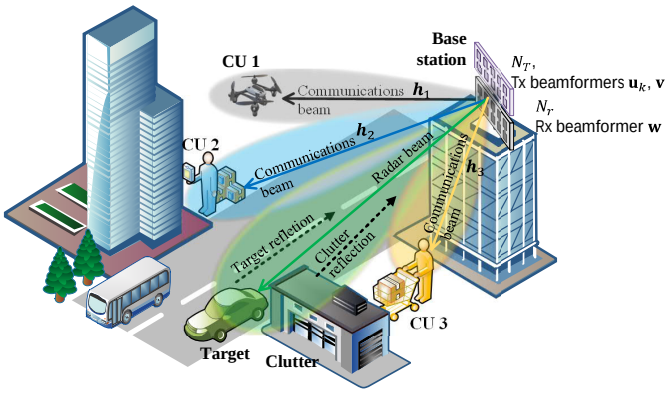

Fig. 1. The presumed multiuser downlink integrated communications and sensing scenario with $K = 3$ CUs.

TABLE I
Important System Parameters and Their Notation.

Parameter	Notation
Transmit antenna	N_T
Receive antenna	N_R
kth CU channel vector	$\mathbf{h}_k$
kth CU data rate requirement	r_k
channel attenuation for target	$\lvert\alpha_0\rvert^2$
channel attenuation for jth clutter	$\lvert\alpha_j\rvert^2$
transmit steering vector at angle θ	$\mathbf{a}_t(\theta)$
transmit steering vector at angle θ	$\mathbf{a}_r(\theta)$
receive combining BF	$\mathbf{w}$
kth CU transmit beamforming vector	$\mathbf{u}_k$
radar probing beamforming vector	$\mathbf{v}$
maximum transmit power	P_{max}

III. System Model and Assumptions

This section presents the main system parameters, underlying assumptions and the important metrics of the considered radar and communication system. We divide this section into multiple subsections on deployment scenario, and performance metrics for communication/radar systems.

A. Deployment scenario

The system model comprises of a multi-antenna DFRC, K single antenna CUs, a radar target located at an angle θ_0 from the DFRC, and J clutter elements where j-th clutter element is located at angle θ_j from the DFRC. A pictorial representation of the considered system model is provided in Fig. 1 and the important system parameters are provided in Table I. The DFRC uses N_t antennas for transmission to the CUs and N_r antennas for reception of target and clutter reflections. The beamformer, and information symbol for k-th CU are denoted by $\mathbf{u}_k \in \mathbb{C}^{N_t \times 1}$, s_k with $E[|s_k|^2] = 1$, respectively. Furthermore, we consider the possibility that the DFRC employs a probing signal with beamforming vector $\mathbf{v} \in \mathbb{C}^{N_t \times 1}$. Hence, the overall transmitted symbol from the DFRC is $\mathbf{x} = \sum_{k=1}^{K} \mathbf{u}_k s_k + \mathbf{v} s_0$, where s_0 with $E[|s_0|^2] = 1$ is the symbol for probing signal. The channel between the

DFRC and k-th CU is represented by $\mathbf{h}_k \in \mathbb{C}^{N_t \times 1}$. Next, we present the performance metrics for communication and radar systems, respectively.

B. Communication system performance metric

With the above assumptions, the received signal at the k-th CU can be written as

$$y_k = \mathbf{h}_k^H \mathbf{u}_k s_k + \sum_{i=1, i\neq k}^{K} \mathbf{h}_k^H \mathbf{u}_i s_i + \mathbf{h}_k^H \mathbf{v} s_0 + \omega_k, \quad (1)$$

where $\omega_k \in \mathbb{C}$ is the additive white Gaussian noise (AWGN) at CU k with zero mean and variance N_0. Therefore, the corresponding SINR is given as

$$\gamma_k^I = \frac{|\mathbf{h}_k^H \mathbf{u}_k|^2}{\sum_{i=1, i\neq k}^{K} |\mathbf{h}_k^H \mathbf{u}_i|^2 + |\mathbf{h}_k^H \mathbf{v}|^2 + N_o}. \quad (2)$$

To meet the essential communications performance r_k of the k-th CU, the data rate for the k-th CU can be obtained through Shannon formula as follows

$$R_k = \log_2\left(1 + \gamma_k^I\right). \quad (3)$$

Therefore, the data rate requirement of the k-th CU can be mathematically represented as

$$\gamma_k^I = \frac{|\mathbf{h}_k^H \mathbf{u}_k|^2}{\sum_{i=1, i\neq k}^{K} |\mathbf{h}_k^H \mathbf{u}_i|^2 + |\mathbf{h}_k^H \mathbf{v}|^2 + N_o} \geq \Gamma_k, \quad (4)$$

where $\Gamma_k = 2^{r_k} - 1$.

C. Radar system performance metric

We present the radar system performance metric for the two scenarios. In the first scenario, we assume that reflected signals from the clutter components can be perfectly removed from the received signal. For this scenario, the radar performance metric is the radar signal to noise ratio (SNR). In the second scenario, we assume that the clutter component cannot be removed from the radar received signal. For this scenario, the radar performance metric is the SCNR.

1) Radar SNR with perfect clutter removal: In the considered system model, the received signal at the radar after the clutter removal can be written as

$$\mathbf{r}^{cr} = \alpha_0 \mathbf{a}_r(\theta_0)\mathbf{a}_t(\theta_0)^H \mathbf{x} + \mathbf{n} = \alpha_0 \mathbf{A}(\theta_0)\mathbf{x} + \mathbf{n}, \quad (5)$$

where $\mathbf{A}(\theta) = \mathbf{a}_r(\theta)\mathbf{a}_t(\theta)^H \in \mathbb{C}^{N_r \times N_t}$, $\alpha_0 \in \mathbb{C}$ is complex channel between target and radar which is independently distributed from $\mathbf{h}_k$'s, $\mathbf{n} \in \mathbb{C}^{N_r \times 1}$ is AWGN with $\mathbf{n} \sim \mathcal{CN}(\mathbf{0}, \mathbf{I})$, $\mathbf{a}_j(\theta) \in \mathbb{C}^{N_j \times 1}$ is the transmit are receive steering vectors for $j \in \{t, r\}$, respectively. The dependencies of the steering vectors $\mathbf{a}_t(\theta), \mathbf{a}_r(\theta)$ on the angle θ are given as

$$\mathbf{a}_t(\theta) = \frac{1}{\sqrt{N_t}}[1, e^{-j2\pi\Delta\sin(\theta)}, \cdots, e^{-j2\pi(N_t-1)\Delta\sin(\theta)}]^H, \quad (6)$$

$$\mathbf{a}_r(\theta) = \frac{1}{\sqrt{N_r}}[1, e^{-j2\pi\Delta\sin(\theta)}, \cdots, e^{-j2\pi(N_r-1)\Delta\sin(\theta)}]^H, \quad (7)$$

where $\Delta = \frac{\lambda}{2}$, and $\lambda = (c/f_c)$ is the carrier wavelength. The radar performs receive beamforming with vector $\mathbf{w}$ on the received signal, then the output of the radar receiver is given as

$$y_r = \mathbf{w}^H \mathbf{r} = \alpha_0 \mathbf{w}^H \mathbf{A}(\theta_0)\mathbf{x} + \mathbf{w}^H \mathbf{n}. \quad (8)$$

Subsequently, the radar SNR can be written as

$$\gamma_r^{cr}(\mathbf{w}) = \frac{|\alpha_0 \mathbf{w}^H \mathbf{A}(\theta_0)\mathbf{x}|^2}{\mathbf{w}^H \mathbf{w}}. \quad (9)$$

The optimal receive beamforming vector that maximizes the radar SNR, is given as

$$\mathbf{w}^* = \frac{\mathbf{A}(\theta_0)\mathbf{x}}{\mathbf{x}^H \mathbf{A}^H(\theta_0)\mathbf{A}(\theta_0)\mathbf{x}}. \quad (10)$$

Putting (10) into (9) we get

$$\gamma_r^{cr}(\mathbf{w}^*) = |\alpha_0|^2 \mathbf{x}^H \mathbf{A}^H(\theta_0)\mathbf{A}(\theta_0)\mathbf{x}, \quad (11)$$

and the corresponding average radar SNR is given as

$$\bar{\gamma}_r^{cr} = |\alpha_0|^2 E\left[\mathbf{x}^H \mathbf{A}^H(\theta_0)\mathbf{A}(\theta_0)\mathbf{x}\right],$$

$$= \sum_{k=1}^{K} \mathbf{u}_k^H \mathbf{\Phi}(\theta_0)\mathbf{u}_k + \mathbf{v}^H \mathbf{\Phi}(\theta_0)\mathbf{v}, \quad (12)$$

where $\mathbf{\Phi}(\theta) = |\alpha_0|^2 \mathbf{A}^H(\theta)\mathbf{A}(\theta)$ with largest eigenvalue ζ_{max} and corresponding eigenvector ϕ.

2) Radar SCNR without clutter removal: For this scenario, the radar received signal with a total of J clutter components can be written as

$$\mathbf{r} = \alpha_0 \mathbf{a}_r(\theta_0)\mathbf{a}_t(\theta_0)^H \mathbf{x} + \sum_{j=1}^{J} \alpha_i \mathbf{a}_r(\theta_j)\mathbf{a}_t(\theta_j)^H \mathbf{x} + \mathbf{n},$$

$$= \alpha_0 \mathbf{A}(\theta_0)\mathbf{x} + \sum_{j=1}^{J} \alpha_j \mathbf{A}(\theta_j)\mathbf{x} + \mathbf{n}, \quad (13)$$

where the target is located at angle θ_0 and the j-th clutter element is located at angle θ_j. Then, after performing the received combining, the radar SCNR can be written as

$$\gamma_r(\mathbf{w}) = \frac{|\alpha_0 \mathbf{w}^H \mathbf{A}(\theta_0)\mathbf{x}|^2}{E\left[\mathbf{w}^H \left(\sum_{j=1}^{J} |\alpha_j|^2 \mathbf{A}(\theta_j)\mathbf{x}\mathbf{x}^H \mathbf{A}^H(\theta_j) + \mathbf{I}\right)\mathbf{w}\right]}. \quad (14)$$

Hence, after performing the expectation operation, we can write $\gamma_r(\mathbf{w})$ as

$$\gamma_r(\mathbf{w}) = \frac{|\alpha_0 \mathbf{w}^H \mathbf{A}(\theta_0)\mathbf{x}|^2}{\mathbf{w}^H \left(\sum_{j=1}^{J} |\alpha_j|^2 \mathbf{A}(\theta_j)\left(\sum_{k=1}^{K} \mathbf{u}_k \mathbf{u}_k^H + \mathbf{v}\mathbf{v}^H\right)\mathbf{A}^H(\theta_j) + \mathbf{I}\right)\mathbf{w}}. \quad (15)$$

The optimal value of $\mathbf{w}$ which maximizes (15) is given as

$$\mathbf{w}^* = \frac{\left(\mathbf{W}(\{\mathbf{u}_k, \mathbf{v}\})\right)^{-1} \mathbf{A}(\theta_0)\mathbf{x}}{\mathbf{x}^H \mathbf{A}^H(\theta_0)\left(\mathbf{W}(\{\mathbf{u}_k, \mathbf{v}\})\right)^{-1} \mathbf{A}(\theta_0)\mathbf{x}}, \quad (16)$$

where

$$\mathbf{W}(\{\mathbf{u}_k, \mathbf{v}\}) = \sum_{j=1}^{J} |\alpha_j|^2 \mathbf{A}(\theta_j)\left(\sum_{k=0}^{K} \mathbf{u}_k \mathbf{u}_k^H + \mathbf{v}\right)\mathbf{A}^H(\theta_j) + \mathbf{I}. \quad (17)$$

Putting (16) into (15), we get

$$\gamma_r(\mathbf{w}^*) = |\alpha_0|^2 \mathbf{x}^H \mathbf{A}^H(\theta_0)\mathbf{W}^{-1}(\{\mathbf{u}_k, \mathbf{v}\})\mathbf{A}(\theta_0)\mathbf{x}, \quad (18)$$

with the corresponding average SCNR given as

$$\bar{\gamma}_r(\mathbf{w}^*) = |\alpha_0|^2 \Bigg[\sum_{k=1}^{K} \mathbf{u}_k^H \mathbf{A}^H(\theta_0)\mathbf{W}^{-1}(\{\mathbf{u}_k, \mathbf{v}\})\mathbf{A}(\theta_0)\mathbf{u}_k + \mathbf{v}^H \mathbf{A}^H(\theta_0)\mathbf{W}^{-1}(\{\mathbf{u}_k, \mathbf{v}\})\mathbf{A}(\theta_0)\mathbf{v} \Bigg]. \quad (19)$$

The detection probability (P_D) of the radar is monotonically increasing with the radar received SNR and SNCR [25], [33], and their mathematical relationship is given as

$$P_D(\gamma_r) = Q\left(\sqrt{2\bar{\gamma}_r}, \sqrt{-2\ln P_{FA}}\right), \quad (20)$$

where P_{FA} is the probability of false-alarm and $Q(.,.)$ is the Marcum Q function. It is clear from equations (4), (12), (19) and (20) that beamformers $\mathbf{u}_k, \mathbf{v}$ determines the communication and radar performance. In the next section, we formulate optimization problems to find the optimal values of $\mathbf{u}_k, \mathbf{v}$.

IV. Optimization framework

We are interested in maximizing the detection probability of the radar. As noted in (20), the radar detection probability is directly proportional to either the radar SNR or the SCNR, depending on the availibility of clutter removal. Our aim is to maximize the radar SNR or SCNR whilst satisfying the SINR requirements of the CUs. The optimization problem for finding the appropriate beamformer for perfect clutter removal scenario is given as follows:

P1:

$$\begin{aligned} \underset{\mathbf{u}_k, \mathbf{v}}{\text{maximize}} \quad & \sum_{k=1}^{K} \mathbf{u}_k^H \mathbf{\Phi}(\theta_0)\mathbf{u}_k + \mathbf{v}^H \mathbf{\Phi}(\theta_0)\mathbf{v} \\ \text{subject to} \quad & C1: \ \frac{|\mathbf{h}_k^H \mathbf{u}_k|^2}{\sum_{i=1, i\neq k}^{K} |\mathbf{h}_k^H \mathbf{u}_i|^2 + |\mathbf{h}_k^H \mathbf{v}|^2 + N_o} \geq \Gamma_k, \\ & C2: \ \sum_{k=1}^{K} |\mathbf{u}_k|^2 + |\mathbf{v}|^2 \leq P_{max}, \end{aligned} \quad (21)$$

and without clutter removal we have:

P2:

$$\begin{aligned} \underset{\mathbf{u}_k, \mathbf{v}}{\text{maximize}} \quad & |\alpha_0|^2 \sum_{k=1}^{K} \mathbf{u}_k^H \mathbf{A}^H(\theta_0)\mathbf{W}^{-1}(\mathbf{x})\mathbf{A}(\theta_0)\mathbf{u}_k \\ & + |\alpha_0|^2 \mathbf{v}^H \mathbf{A}^H(\theta_0)\mathbf{W}^{-1}(\mathbf{x})\mathbf{A}(\theta_0)\mathbf{v} \\ \text{subject to} \quad & C1, C2. \end{aligned} \quad (22)$$

The objective of **P1**, **P2** is to maximize the average SNR, SCNR of the radar system, respectively. The constraints $C1$ guarantee that data rate requirements of the CUs are met and $C2$ ensures that the total transmitted power is no more than the maximum allowed transmit power. For **P1**, the objective is a convex function and the constraints $C1$ are non-convex which make **P1** a non-convex optimization problem and hence difficult to solve. For **P2**, the constraints are non-convex. Although both problems **P1**, **P2** are non-convex, in the following we show that problem **P1** can be solved optimally and the globally optimal solution can be presented in closed-form. On the other hand, an iterative algorithm with guaranteed convergence is proposed to find a suboptimal solution for problem **P2**.

A. Proposed solution for problem *P1*

To solve **P1**, we use the semidefinite relaxation (SDR) technique. In this regard, we introduce the following variables $\mathbf{U}_k = \mathbf{u}_k \mathbf{u}_k^H, \mathbf{V} = \mathbf{v}\mathbf{v}^H$, and constants $\mathbf{H}_k = \mathbf{h}_k \mathbf{h}_k^H$. Then, **P1** can be equivalently written as

P1-equ:

$$\begin{aligned} \underset{\mathbf{U}_k, \mathbf{V}}{\text{maximize}} \quad & \sum_{k=1}^{K} \mathrm{Tr}(\mathbf{\Phi}\mathbf{U}_k) + \mathrm{Tr}(\mathbf{\Phi}\mathbf{V}) \\ \text{subject to} \quad & \tilde{C1}: \ \frac{\mathrm{Tr}(\mathbf{H}_k \mathbf{U}_k)}{\mathrm{Tr}\left(\mathbf{H}_k \left(\sum_{i=1, i\neq k}^{K} \mathbf{U}_i + \mathbf{V}\right)\right) + N_o} \geq \Gamma_k, \\ & \tilde{C2}: \ \sum_{k=1}^{K} \mathrm{Tr}(\mathbf{U}_k) + \mathrm{Tr}(\mathbf{V}) \leq P_{max}, \\ & \tilde{C3}: \ \mathbf{U}_k \succeq \mathbf{0}, \\ & \tilde{C4}: \ \mathbf{V} \succeq \mathbf{0}, \\ & \tilde{C5}: \ \mathrm{rank}(\mathbf{U}_k) \leq 1, \\ & \tilde{C6}: \ \mathrm{rank}(\mathbf{V}) \leq 1, \end{aligned} \quad (23)$$

where for simplicity of notation, we have used $\mathbf{\Phi}(\theta) = \mathbf{\Phi}$. **P1-equ** is non-convex as constraints $\tilde{C5}$, $\tilde{C6}$ are non-convex. However, if we remove the constraints $\tilde{C5}$, $\tilde{C6}$, the relaxed problem is a semi-definite program (SDP), whose solution can be easily found through tools such as CVX.

After relaxing the constraints $\tilde{C5}$, $\tilde{C6}$ in **P2**, we denote the new problem as **P2-rel** given as

P1-rel:

$$\begin{aligned} \underset{\mathbf{U}_k, \mathbf{V}}{\text{maximize}} \quad & \sum_{k=1}^{K} \mathrm{Tr}(\mathbf{\Phi}\mathbf{U}_k) + \mathrm{Tr}(\mathbf{\Phi}\mathbf{V}) \\ \text{subject to} \quad & \tilde{C1}: \ \frac{\mathrm{Tr}(\mathbf{H}_k \mathbf{U}_k)}{\mathrm{Tr}\left(\mathbf{H}_k \left(\sum_{i=1, i\neq k}^{K} \mathbf{U}_i + \mathbf{V}\right)\right) + N_o} \geq \Gamma_k, \\ & \tilde{C2}: \ \sum_{k=1}^{K} \mathrm{Tr}(\mathbf{U}_k) + \mathrm{Tr}(\mathbf{V}) \leq P_{max}, \\ & \tilde{C3}: \ \mathbf{U}_k \succeq \mathbf{0}, \\ & \tilde{C4}: \ \mathbf{V} \succeq \mathbf{0} \end{aligned} \quad (24)$$

Then, Lemma 1 below provides a useful result about **P1-rel**.

Lemma 1. *The optimal solution of **P1-rel** has following properties*

- $\mathrm{rank}(\mathbf{U}_k^*) = 1$,
- $\mathbf{V}^* = \mathbf{0}$.

Proof. Please see Appendix A for the proof. □

Remark 1. *Lemma 1 shows that the obtained solution for **P1-rel** is the optimal solution for **P1**. This lemma also helps*

in reducing the complexity of finding solution by reducing the number of optimization variables through noting that $\mathbf{V}^* = \mathbf{0}$. According to Proposition 1, the idea is to avoid that part of the interference at the CUs which is caused by the probing signal. This is because the probing signal cannot be cancelled at the CUs as they do not have the a priori *information about the radar probing signal waveform. Thus, the optimal transmission strategy is to adjust the beamforming for the CUs only in such a way that the radar SNR is maximized.*

In the rest of this subsection, we assume that $\mathbf{v}^* = \mathbf{0}$ based on Lemma 1. Next, we use results presented above to find a closed-form solution for the optimization problem **P1**. The Lagrangian of **P1** with $\mathbf{v}^* = \mathbf{0}$ can be written as

$$\mathcal{L}(\mathbf{u}_k, \eta_k, \omega) = -\sum_{k=1}^{K} \mathbf{u}_k^H \mathbf{\Phi} \mathbf{u}_k + \omega(\sum_{k=1}^{K} |\mathbf{u}_k|^2 - P_{max}) + \sum_{k=1}^{K} \eta_k \left(\Gamma_k \sum_{i=1, i\neq k}^{K} |\mathbf{h}_k^H \mathbf{u}_i|^2 + \Gamma_k N_o - |\mathbf{h_k}^H \mathbf{u}_k|^2 \right), \tag{25}$$

and the corresponding dual problem can be written as

P1-d:

$$\underset{\eta_k, \omega}{\text{maximize}} \quad \min_{\mathbf{u}_k} \mathcal{L}(\mathbf{u}_k, \eta_k, \omega). \tag{26}$$

The following lemma presents a useful result for the problem **P1**, **P1-d**.

Lemma 2. *The optimal values of **P1**, **P1-d** are equal i.e. the duality gap for problem **P1** is zero.*

Proof. Please refer to Appendix B for the proof. □

Based on Lemma 2, we can solve **P1-d** to obtain the solution of **P1** in closed-form. Then, we present an important property of the solution for problem **P1** in the following lemma.

Lemma 3. *Problem **P1** has following property.*

- *If $\mathbf{u}_k^*, \forall k \in \{1, \cdots K\}$ is the optimal solution of problem **P1**, then $\mathbf{u}_k^* e^{j\theta_k}$ is also an optimal solution for problem **P1**.*

Proof. The proof is given in Appendex C. □

With the help of Lemma 2 and Lemma 3, we can obtain the optimal solution of the problem $\min_{\mathbf{u}_k} \mathcal{L}(\mathbf{u}_k, \eta_k, \omega)$ in the following lemma.

Lemma 4. *The optimal solution of $\min_{\mathbf{u}_k} \mathcal{L}(\mathbf{u}_k, \eta_k, \omega)$ for any given ω, η_k is*

$$\mathbf{u}_k^*(\omega, \{\eta_k\}) = \sqrt{p_k} \frac{\left[\omega \mathbf{I} - \mathbf{\Phi} + \sum_{i=1, i\neq k}^{K} \eta_i \mathbf{h}_i \mathbf{h}_i^H\right]^{-1} \mathbf{h}_k}{\left\| \left[\omega \mathbf{I} - \mathbf{\Phi} + \sum_{i=1, i\neq k}^{K} \eta_i \mathbf{h}_i \mathbf{h}_i^H\right]^{-1} \mathbf{h}_k \right\|}, \tag{27}$$

where

$$p_k = \frac{\Gamma_k \mathbf{h}_k^H \left(\sum_{i=1, i\neq k}^{K} p_i \hat{\mathbf{u}}_i \hat{\mathbf{u}}_i^H \right) \mathbf{h}_k + \Gamma_k N_0}{|\mathbf{h}_k^H \hat{\mathbf{u}}_k|^2}, \tag{28}$$

and

$$\hat{\mathbf{u}}_k = \frac{\left[\omega \mathbf{I} - \mathbf{\Phi} + \sum_{i=1, i\neq k}^{K} \eta_i \mathbf{h}_i \mathbf{h}_i^H\right]^{-1} \mathbf{h}_k}{\left\| \left[\omega \mathbf{I} - \mathbf{\Phi} + \sum_{i=1, i\neq k}^{K} \eta_i \mathbf{h}_i \mathbf{h}_i^H\right]^{-1} \mathbf{h}_k \right\|}. \tag{29}$$

Proof. Please refer to Appendix D for the proof. □

Remark 2. *There is an intuitive explanation associated with the transmit beamforming expression for k-th CU in (27). First, it is expected that the transmit beamforming for k-th CU should be aligned with $\mathbf{h}_k$. This is reflected by the presence of $\mathbf{h}_k$ in the numerator of (27). Second, the transmit beamforming of the k-th CU is expected to reduce interference to other CUs. This is reflected by the term $\sum_{i=1, i\neq k}^{K} \mathbf{h}_i \mathbf{h}_i^H$ within the inverse matrix in the numerator. Thirdly, the transmit beamforming for the k-th CU must try to direct energy toward the target direction. This is achieved by the inclusion of $-\mathbf{\Phi}$ within the inverse matrix in the numerator of (27).*

Remark 3. *The relationship depicted in (28) also alludes to another important characteristic of the proposed solution. Specifically, (28) reflects the fact that if the problem **P1** is feasible, then only minimum required power to satisfy the SINR constraints of CUs will be directed toward CUs. Thus, the remaining power is available for directing towards the target as explained in Remark 1. This behavior suggests that proposed schemes efficiently use the available power for full filling both radar and communication performances.*

Also, we can use the gradient descent method to find the optimal values of $\omega, \{\eta_k\}$ as follows

$$\omega^{i+1} = \omega^i + \Xi_\omega (\sum_{k=1}^{K} |\mathbf{u}_k(\omega^i, \eta_k^i)|^2 - P_{max}), \tag{30}$$

$$\eta_k^{i+1} = \eta_k^i + \Xi_{\eta_k} \left(\Gamma_k \sum_{i=1, i\neq k}^{K} |\mathbf{h}_k^H \mathbf{u}_i(\omega^i, \eta_k^i)|^2 + \Gamma_k N_o - |\mathbf{h_k}^H \mathbf{u}_k(\omega^i, \eta_k^i)|^2 \right), \tag{31}$$

where Ξ_ω, and Ξ_{η_k} are step sizes for update of ω, η_k in subgradient algorithm, respectively. With above analysis, the proposed algorithm for solving **P1** is given as **Algorithm 1**. Furthermore, to assess the computational simplification of Algorithm 1, we consider its computational complexity and compare it against that of SDR technique. The computational complexity of the SDR technique for solving P1 is proportional to $\mathcal{O}(\max(K, N_t)^4 N_t^{\frac{1}{2}})$ [40]. Since the Algorithm 1 uses gradient descent method to calculate dual variables, the complexity is dominated by the matrix inversion operation. Thus, Algorithm 1 needs to perform $\mathcal{O}(N_t^3)$ operations for matrix inversion to calculate (27), and therefore the computational complexity of Algorithm 1 is $\mathcal{O}(N_t^3)$.

Algorithm 1: Proposed alternating optimization algorithm for solving **P1**.

Initialize: $i = 0, \epsilon, i_{max}, \mathbf{\Phi}, \mathbf{h}_k, \forall k \in \{1, \cdots, K\}$, $\mathbf{A}(\theta_0), \mathbf{A}(\theta_i), \forall i \in \{1, \cdots, I\}, \eta_k^i, \omega^i,$.
Calculate $\mathbf{u}_k(\eta_k^i, \omega^i)$ using (27).
Calculate $f(i) = \mathbf{u}_k^H(\eta_k^i, \omega^i)\mathbf{\Phi}\mathbf{u}_k(\eta_k^i, \omega^i)$.
while $i \leq i_{max}$ **do**
  Set $i = i + 1$
  Update the values of η_k^i through subgradient method.
  Update the value of ω^i through subgradient method.
  Calculate $f(i) = \mathbf{u}_k^H(\eta_k^i, \omega^i)\mathbf{\Phi}\mathbf{u}_k(\eta_k^i, \omega^i)$
  if $f(i) - f(i-1) \leq \epsilon$ **then**
    $\mathbf{u}_k^* = \mathbf{u}_k(\eta_k^i, \omega^i)$,
    Break
  end if
end while

B. Proposed solution for problem P2

When clutter removal is not possible, the objective function becomes more complex than that of problem **P1** due to the involvement of

$$\mathbf{W}(\{\mathbf{u}_k,\mathbf{v}\}) = \sum_{j=1}^{J} |\alpha_j|^2 \mathbf{A}(\theta_j) \left(\sum_{k=1}^{K} \mathbf{u}_k \mathbf{u}_k^H + \mathbf{v}\mathbf{v}^H \right) \mathbf{A}^H(\theta_j) + \mathbf{I}. \quad (32)$$

To address this issue, we use an iterative approach where in each iteration the optimization variables $\{\mathbf{u}_k, \mathbf{v}\}$ in $\mathbf{W}(\{\mathbf{u}_k, \mathbf{v}\})$ are replaced by optimal values of $\{\mathbf{u}_k, \mathbf{v}\}$ computed in the previous iteration. Hence, in the $l+1$-th iteration we set

$$\begin{aligned} \mathbf{\Phi}' &= \mathbf{A}^H(\theta_0)(\mathbf{W}(\{\mathbf{u}_k, \mathbf{v}\})^{-1}\mathbf{A}(\theta_0) \\ &= \mathbf{A}^H(\theta_0)(\mathbf{W}(\{\mathbf{u}_k^l, \mathbf{v}^l\})^{-1}\mathbf{A}(\theta_0), \end{aligned} \quad (33)$$

where $\{\mathbf{u}_k^l, \mathbf{v}^l\}$ is the optimal solution achieved in the l-th iteration. The iterative procedure is repeated until a sufficient convergence criteria is met or the maximum number of iterations is reached. Therefore, during the $l+1$-th iteration the optimization problem **P2** is modified as

P2':

$$\begin{aligned} \underset{\mathbf{u}_k, \mathbf{v}}{\text{maximize}} \quad & |\alpha_0|^2 \sum_{k=1}^{K} \mathbf{u}_k^H \mathbf{\Phi}' \mathbf{u}_k + |\alpha_0|^2 \mathbf{v}^H \mathbf{\Phi}' \mathbf{v} \\ \text{subject to} \quad & C1: \ \frac{|\mathbf{h}_k^H \mathbf{u}_k|^2}{\sum_{i=1, i\neq k}^{K} |\mathbf{h}_k^H \mathbf{u}_i|^2 + |\mathbf{h}_k^H \mathbf{v}|^2 + N_o} \geq \Gamma_k, \\ & C2: \ \sum_{k=1}^{K} |\mathbf{u}_k|^2 + |\mathbf{v}|^2 \leq P_{max}, \end{aligned} \quad (34)$$

with the corresponding SDR relaxation given as

P2'-SDR:

$$\begin{aligned} \underset{\mathbf{U}_k, \mathbf{V}}{\text{maximize}} \quad & \sum_{k=1}^{K} \text{Tr}(\mathbf{\Phi}'\mathbf{U}_k) + \text{Tr}(\mathbf{\Phi}'\mathbf{V}) \\ \text{subject to} \quad & \tilde{C}1 - \tilde{C}4. \end{aligned} \quad (35)$$

In each iteration, optimal solutions depend on the channel gains h_k's of the CUs, which can cause dependence of $\mathbf{\Phi}'$ on the channel gains. Thus, the independence argument used in the proof of Lemma 1 cannot be used here for showing that $\text{rank}(\mathbf{U}_k^*) = 1$. In this case, the following lemma presents the solution structure for problem **P2'-SDR**.

Lemma 5. *There exists an optimal solution for **P2'-SDR** such that*

- $\mathbf{V}^* = \mathbf{0}$,
- $\text{rank}(\mathbf{U}_k^*) = 1$.

Proof. Please see the Appendix E for proof. □

Therefore, we can use $\mathbf{v}^* = \mathbf{0}$. Hence, the objective function for problem **P2'** becomes $|\alpha_0|^2 \sum_{k=1}^{K} \mathbf{u}_k^H \mathbf{\Phi}' \mathbf{u}_k$. Also using the arguments similar to Lemma 2, it can be established that the duality gap between **P2** and **P2-d** is zero, where **P2-d** is the dual problem corresponding to the primal problem **P2**. Then, the closed-form solution for problem **P2** is given as

$$\mathbf{v}^* = \mathbf{0},$$

$$\mathbf{u}_k^*(\omega', \{\eta_k'\}) = \frac{\sqrt{p_k} \left[\omega' \mathbf{I} - \mathbf{\Phi}' + \sum_{i=1, i\neq k}^{K} \eta_i' \mathbf{h}_i \mathbf{h}_i^H \right]^{-1} \mathbf{h}_k}{\left\| \left[\omega' \mathbf{I} - \mathbf{\Phi}' + \sum_{i=1, i\neq k}^{K} \eta_i' \mathbf{h}_i \mathbf{h}_i^H \right]^{-1} \mathbf{h}_k \right\|} \quad (36)$$

where

$$p_k' = \frac{\Gamma_k \mathbf{h}_k^H \left(\sum_{i=1, i\neq k}^{K} p_i' \hat{\mathbf{u}}_i' \hat{\mathbf{u}}_i'^H \right) \mathbf{h}_k + \Gamma_k N_0}{|\mathbf{h}_k^H \hat{\mathbf{u}}_k'|^2}, \quad (37)$$

$$\hat{\mathbf{u}}_k' = \frac{\left[\omega' \mathbf{I} - \mathbf{\Phi}' + \sum_{i=1, i\neq k}^{K} \eta_i' \mathbf{h}_i \mathbf{h}_i^H \right]^{-1} \mathbf{h}_k}{\left\| \left[\omega' \mathbf{I} - \mathbf{\Phi}' + \sum_{i=1, i\neq k}^{K} \eta_i' \mathbf{h}_i \mathbf{h}_i^H \right]^{-1} \mathbf{h}_k \right\|}, \quad (38)$$

and $\omega', \{\eta_k'\}$ are the dual variables corresponding to the maximum transmit power constraint and the SINR constraints in problem **P2**.

Remark 4. *The mathematical formulation of the transmit beamforming of the k-th CU can be intuitively explained as follows. First, the transmit beamforming of k-th CU should align with $\mathbf{h}_k$. This is reflected by the term $\mathbf{h}_k$ in the numerator of (36). Second, the transmit beamforming of the k-th CU should reduce interference to other CUs. This is reflected by the term $\sum_{i=1, i\neq k}^{K} \mathbf{h}_i \mathbf{h}_i^H$ within the inverse matrix in the numerator. Thirdly, the transmit beamforming of k-th CU must try to direct energy toward the target direction. This is achieved by the inclusion of $-\mathbf{\Phi}'$, and its dependence on $\mathbf{A}(\theta_0)$, within the inverse matrix in the numerator of (36). Lastly, the transmit beamforming of the k-th CU should avoid directing energy toward the clutter. This is reflected by the presence of $(\mathbf{W}(\{\mathbf{u}_k\}))^{-1}$, and its dependence on $\mathbf{A}(\theta_i)$, within $\mathbf{\Phi}'$ in the inverse matrix.*

The iterative algorithm for solving **P2** is presented in **Algorithm 2**. Moreover, the optimal values of $\omega', \{\eta_k'\}$ can be found in an iterative manner using update rules suggested in (30), (31).

To assess the computational savings of Algorithm 2, we consider its worst case situation and compare it against that of SDR. In worst case, we assume that the outer iteration in

Algorithm 2: Proposed alternating optimization algorithm for solving **P2**.

Initialize: $i = 0, j = 0, \epsilon_1, \epsilon_2, i_{max}, j_{max}$, $\mathbf{u}_k, \mathbf{h}_k, \forall k \in \{1, \cdots, K\}$, $\mathbf{A}(\theta_0), \mathbf{A}(\theta_i), \forall i \in \{1, \cdots, I\}, \eta_k'^j, \omega'^j$.
Calculate $\mathbf{u}_k = \mathbf{u}_k(\eta_k'^j, \omega'^j)$ using (36).
Calculate $\mathbf{\Phi'(i)}$ using (33).
Calculate $f(i,0) = \mathbf{u}_k^H \mathbf{\Phi'}(i)\mathbf{u}_k$.
while $i \leq i_{max}$ **do**
  Set $i = i + 1$
  while $j \leq j_{max}$ **do**
    Set $j = j + 1$
    Update $\eta_k'^j$ through subgradient method.
    Update ω'^j through subgradient method.
    Calculate $f(i,j) = \mathbf{u}_k^H(\eta_k'^j, \omega'^j)\mathbf{\Phi'}(i)\mathbf{u}_k(\eta_k'^j, \omega'^j)$
    if $f(i,j) - f(i,j-1) \leq \epsilon_1$ **then**
      Set $\mathbf{u}_k^{i*} = \mathbf{u}_k(\eta_k'^j, \omega'^j)$,
      Set $j = 0$
      Break
    end if
  end while
  if $\mathbf{u^H}_k^{i*} \mathbf{\Phi'}(i)\mathbf{u}_k^{i*} - \mathbf{u^H}_k^{(i-1)*} \mathbf{\Phi'}(i-1)\mathbf{u}_k^{(i-1)*} \leq \epsilon_2$ **then**
    $\mathbf{u}_k^* = \mathbf{u}^{i*}$
    Break
  end if
end while

Algorithm is run i_{max} times and the inner iteration is run j_{max} times. For both techniques, in each outer iteration, first a matrix inversion is required to compute $\mathbf{\Phi'}$ which needs $\mathcal{O}(N_t^3)$ operations. Then, in each inner iteration, the computational complexity is proportional to $\mathcal{O}(\max(K, N_t)^4 N_t^{\frac{1}{2}})$ [40] for the SDR technique. For Algorithm 2, the complexity is dominated by the matrix inversion. Thus, Algorithm 2 needs to perform $\mathcal{O}(N_t^3)$ operations for matrix inversion to calculate the values of $\mathbf{u}_k$ through (36), and therefore the complexity of Algorithm 2 in each inner iteration is $\mathcal{O}(N_t^3)$. Therefore, the worst case complexity for the SDR based technique is $\mathcal{O}\left(i_{max}\left(N_r^3 + j_{max}\left(\max(K, N_t)^4 N_t^{\frac{1}{2}}\right)\right)\right)$, while for Algorithm 2 it is $\mathcal{O}(i_{max}\left(N_r^3 + j_{max} N_t^3\right)$.

The above algorithm works in the iterative manner, the complexity for finding the solution in each iteration determines the total algorithm complexity. The main computationally extensive operation is finding the inverse matrix for $\mathbf{W}(\{\mathbf{u}_k\})$, in the calculation of $\mathbf{\Phi'}$, for which the complexity increases in cubic fashion with its size. Specifically, for a square matrix of size N the computational complexity for finding its inverse is $\mathcal{O}(N^3)$. For large number of antennas, this results in significant complexity rise. The next section provides an iterative low complexity algorithm.

V. Low complexity algorithms for solving the optimization problem

As mentioned above, the main bottleneck of finding solution lies in finding the inverse matrix of $\mathbf{W}(\{\mathbf{u}_k\})$. In this section, we provide approximation for this matrix which helps in reducing the complexity for finding its inverse. To this end, we make use of the following lemma.

Lemma 6. *Matrix $\mathbf{W}(\{\mathbf{u}_k\})$ is a Toeplitz matrix, where a general square Topelitz matrix $\mathbf{S}$ of size N has following form:*

$$\mathbf{S} = \begin{bmatrix} s(0) & s(-1) & s(-2) & \cdots & s(-(N-1)) \\ s(1) & s(0) & s(-1) & & \\ s(2) & s(1) & s(0) & & \vdots \\ \vdots & & & \ddots & \\ s(N-1) & & \cdots & & s(0) \end{bmatrix}, \tag{39}$$

or $\mathbf{S}[m,n] = s(m-n); m, n \in \{0, 1, \cdots, N-1\}$.

Proof. The proof is given in Appendix F. □

Next, since Toeplitz matrices can be efficiently approximated by Circulant matrices, we represent $\mathbf{W}(\{\mathbf{u}_k\})$ by its Circulant matrix approximation $\mathbf{C}$ where the top row entries of $\mathbf{C}$ are obtained as follows

$$c_1 = \mathbf{W}_{1,1}, \quad c_i = \mathbf{W}_{1,i} + \mathbf{W}_{N-i+2,1}, \forall\ i \in \{2, \cdots N\}. \tag{40}$$

Next, we state an important property of the Hermitian Circulant matrices in the following lemma.

Lemma 7. *If $\mathbf{X}$ is a Hermitian Circulant matrix then its inverse $\mathbf{X}^{-1}$ is also a Hermitian Circulant matrix.*

Proof. The proof is provided in Appendix G. □

Then, we can use the following lemma to approximate the objective function of **P2**.

Lemma 8. *The objective function of **P2**, $|\alpha_0|^2 \sum_{k=1}^K \mathbf{u}_k^H \mathbf{\Phi'} \mathbf{u}_k$, can be approximated as*

$$|\alpha_0|^2 \sum_{k=1}^K \mathbf{u}_k^H \mathbf{\Phi'} \mathbf{u}_k \simeq |\alpha_0|^2 \sum_{k=1}^K \tilde{\mathbf{u}}_k^H \tilde{\mathbf{\Lambda}} \tilde{\mathbf{u}}_k, \tag{41}$$

where $a \simeq b$ means $\lim_{N_r \to \infty}(a - b) \leq 0 \Rightarrow \lim_{N_r \to \infty}(a - b) = 0$, $\tilde{\mathbf{\Lambda}}$ is a diagonal matrix and

$$\tilde{\mathbf{u}}_k = \mathbf{F}\mathbf{A}(\theta_0)\mathbf{u}_k, \tag{42}$$

with $\mathbf{F}$ being the unitary DFT matrix.

Proof. Please refer to the Appendix H for the proof. □

With the help of Lemma 8, we can modify **P2** as follows:

P2':

$$\begin{aligned} \underset{\mathbf{u}_k, \mathbf{v}}{\text{maximize}} \quad & |\alpha_0|^2 \sum_{k=1}^K \tilde{\mathbf{u}}_k^H \tilde{\mathbf{\Lambda}} \tilde{\mathbf{u}}_k + \tilde{\mathbf{v}}^H \tilde{\mathbf{\Lambda}} \tilde{\mathbf{v}} \\ \text{subject to} \quad & C1, C2, \end{aligned} \tag{43}$$

where $\tilde{\mathbf{v}} = \mathbf{F}\mathbf{A}(\theta_0)\mathbf{v}$.

Using the results discussed in the previous section, we can devise an iterative algorithm for solving **P2'**. The optimal solutions in each iteration are given in the following corollary.

Corollary 1. *The optimal solution for **P2'** in the i-th iteration is given as*

$$\tilde{\mathbf{v}}^* = \mathbf{0}, \tag{44}$$

TABLE II
SIMULATION PARAMETERS.

Parameter	value	Parameter	value
f_c	3.5 GHz	Bandwidth	100 MHz
N_0	-94	Propagation	UMi [22]
N_t	$\{8, 12, 16, 24, 32\}$	N_R	$\{8, 12, 16, 24, 32\}$
K	4	Γ_k	$[5, 25]$ dB
P_{max}	30 dBm	d_1^{CU}	10 m
d_2^{CU}	15 m	d_3^{CU}	20 m
d_4^{CU}	25 m	J	2
$\lvert\alpha_1\rvert^2$	.01	$\lvert\alpha_2\rvert^2$	.001
θ_0	$\frac{\pi}{4}$	θ_1	0
θ_2	$\frac{\pi}{2}$	P_{FA}	$\{10^{-5}, 10^{-6}\}$

$$\tilde{\mathbf{u}}_k^*(\tilde{\omega}, \{\tilde{\eta}_k\}) = \sqrt{p_k} \frac{\left[\tilde{\omega}\mathbf{I} - \tilde{\mathbf{\Phi}} + \sum_{i=1, i\neq k}^{K} \tilde{\eta}_i \mathbf{h}_i \mathbf{h}_i^H\right]^{-1} \mathbf{h}_k}{\left\| \left[\tilde{\omega}\mathbf{I} - \tilde{\mathbf{\Phi}} + \sum_{i=1, i\neq k}^{K} \tilde{\eta}_i \mathbf{h}_i \mathbf{h}_i^H\right]^{-1} \mathbf{h}_k \right\|}, \tag{45}$$

where

$$\tilde{p}_k = \frac{\Gamma_k \mathbf{h}_k^H \left(\sum_{i=1, i\neq k}^{K} \tilde{p}_i \tilde{\mathbf{u}}_i \tilde{\mathbf{u}}_i^H\right) \mathbf{h}_k + \Gamma_k N_0}{|\mathbf{h}_k^H \hat{\mathbf{u}}_k|^2}, \tag{46}$$

$$\tilde{\mathbf{u}}_k = \frac{\left[\tilde{\omega}\mathbf{I} - \tilde{\mathbf{\Phi}} + \sum_{i=1, i\neq k}^{K} \tilde{\eta}_i \mathbf{h}_i \mathbf{h}_i^H\right]^{-1} \mathbf{h}_k}{\left\| \left[\tilde{\omega}\mathbf{I} - \tilde{\mathbf{\Phi}} + \sum_{i=1, i\neq k}^{K} \tilde{\eta}_i \mathbf{h}_i \mathbf{h}_i^H\right]^{-1} \mathbf{h}_k \right\|}, \tag{47}$$

$$\tilde{\mathbf{\Phi}} = \mathbf{A}^H(\theta_0) \mathbf{F}^H \tilde{\mathbf{\Lambda}}^{-1} \mathbf{F} \mathbf{A}(\theta_0), \tag{48}$$

*and $\tilde{\omega}, \{\tilde{\eta}_k\}$ are the dual variables corresponding to the maximum transmit power constraint and SINR constraints in problem **P2'**.*

Proof. The proof follows similar reasoning as described in Section V and hence omitted. □

We can use **Algorithm 2** for solving **P2'** by exchanging $\mathbf{\Phi}'$ with $\tilde{\mathbf{\Phi}}$. In finding $\tilde{\mathbf{\Phi}}$ we need to find the eigenvalues of a Circulant matrix. Thus, the main complexity in the outer loop is due to the calculations needed for eigenvalue computations. It is known that the eigenvalue computation for a Circulant matrix of size N_r need $\mathcal{O}(N_r \log(N_r))$ operations. Therefore, the computational complexity for solving problem **P2'** in the worst case is $\mathcal{O}(i_{max}\left(N_r \log(N_r) + j_{max} N_t^3\right))$.

VI. NUMERICAL RESULTS

In this section, we provide example simulation results. The important simulation parameters are provided in Table II. For performance comparison with other schemes, we consider two baseline schemes: (i) radar centric and (ii) communication centric.

A. Radar centric scheme

In the radar centric scheme, the objective is to maximize the radar SCNR, while neglecting the SINR constraints of the communication users. Mathemtically, the optimization problem for radar centric scheme can be written as follow

$$\begin{aligned} \underset{\mathbf{v}}{\text{maximize}} \quad & |\alpha_0|^2 \mathbf{v}^H \mathbf{A}^H(\theta_0) \mathbf{W}^{-1}(\mathbf{v}) \mathbf{A}(\theta_0) \mathbf{v} \\ \text{subject to} \quad & \|\mathbf{v}\|^2 \leq P_{max}. \end{aligned} \tag{49}$$

The problem (49) is solved by using the proposed iterative algorithm but without consideration of the CUs' SINR constraints. Henceforth, this scheme is referred to as the radar SCNR maximization (RSM) scheme.

B. Communication centric scheme

On the other hand, in the communication centric scheme, the objective is to minimize the total consumed power while satisfying the SINR requirements of all the CUs. Mathematically, the communication centric optimization problem can be written as

$$\begin{aligned} \underset{\mathbf{u}_k}{\text{minimize}} \quad & \sum_{k=1}^{K} \|\mathbf{u}_k\|^2 \\ \text{subject to} \quad & \frac{|\mathbf{h}_k^H \mathbf{u}_k|^2}{\sum_{i=1, i\neq k}^{K} |\mathbf{h}_k^H \mathbf{u}_i|^2 + N_o} \geq \Gamma_k. \end{aligned} \tag{50}$$

In the following, this scheme is termed as communication power minimization (CPM) scheme. The achieved radar SCNR for the CPM scheme is obtained as

$$SCNR_{CPM} = |\alpha_0|^2 \sum_{k=1}^{K} \mathbf{u}_{k,c}^H \mathbf{A}^H(\theta_0) \mathbf{W}^{-1}(\mathbf{u}_{k,c}) \mathbf{A}(\theta_0) \mathbf{u}_{k,c}, \tag{51}$$

where the vector $\mathbf{u}_{k,c}$'s is the optimal transmit beamformer of CU k for problem (50). For (50), the optimal solution for CPM problem satisfy the SINR constraints with equality [41].

In the following, first we show the effect of clutter removal on the radar SCNR for different number of N_t, N_r. Second, we compare the proposed scheme with RSM and CPM schemes. Then, we compare the proposed scheme and the proposed low complexity algorithm.

C. Results

Fig. 2 presents the effect of clutter removal on the SCNR maximization of the proposed algorithms. It can be observed that the clutter removal operation at the DFRC BS can substantially enhance the SCNR for radar. This behavior can be understood through optimal solution expressions for transmit beamformers of CUs, where it is noted that the optimal beamformers for clutter removal scenario does not take clutter into account while assigning beamforming weights for CUs. Thus, less power being directed toward CUs may satisfy their SINR requirements which effectively allows more power to be directed toward the target. This leads to a higher SCNR as compared to the no clutter removal scenario. Moreover, it can be observed that for higher values of required SINR for CUs, the radar SCNR reduces. It is due to the higher directional gain requirement toward the CUs to meet their larger SINR constraints. These effects are in agreement with the statements made in Remark 2 and 3.

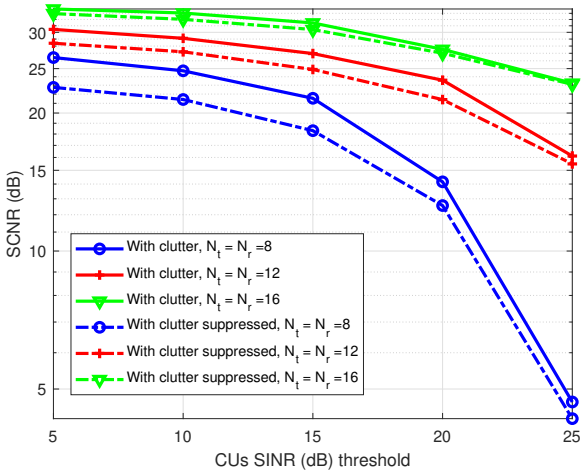

Fig. 2. Effect of clutter suppression.

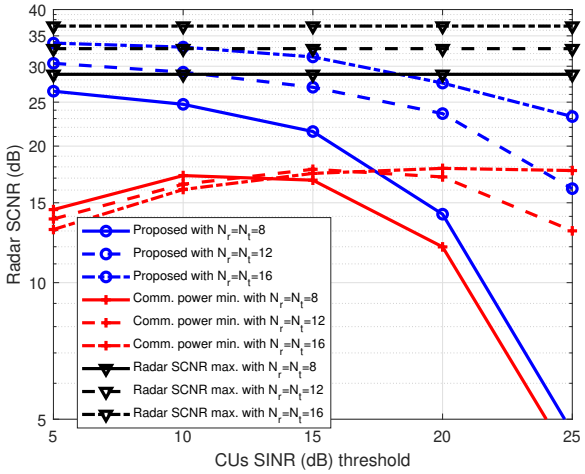

Fig. 3. Comparison with CPM and RSM.

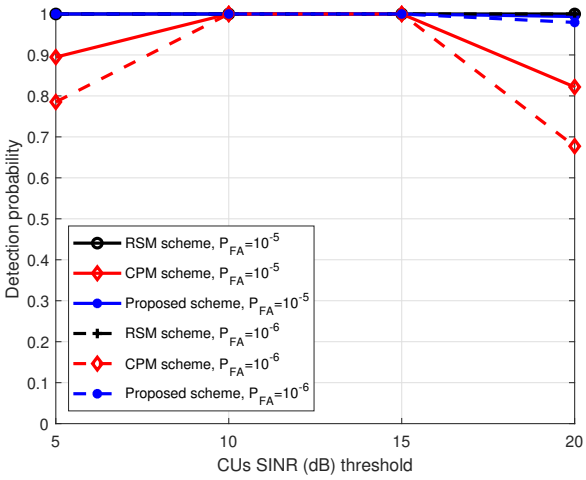

Fig. 4. Detection probability with respect to CUs SINR requirements for different P_{FA}.

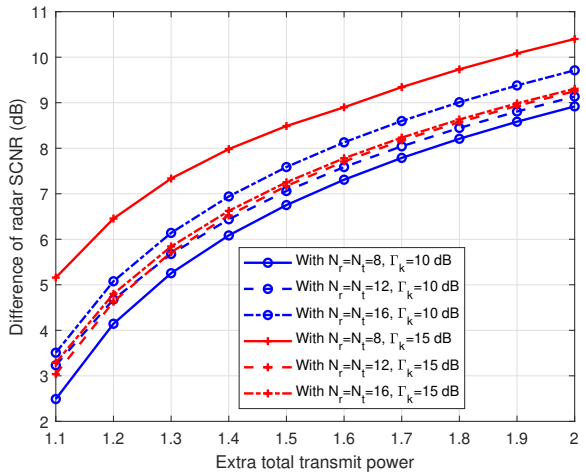

Fig. 5. Improvement in radar SCNR as a result of increased total transmit power.

In Fig. 3, we compare radar SCNR performances of the proposed scheme, RSM and CPM schemes. *First*, we can see that RSM outperforms other schemes. This is expected since every feasible solution of problem **P2** obtained through the proposed iterative algorithms is also a feasible solution for the RSM problem. Thus, the feasible region of solutions for the RSM problem is larger, which results in a higher achievable SCNR for the RSM scheme as compared to the proposed scheme. However, we can see that for lower SINR region of CUs, the performance of the proposed scheme is identical to the RSM scheme. This is due to the fact that at lower SINR region, a smaller power directed toward the CUs can satisfy their SINR requirements thus leaving a higher portion of transmit power available for the target detection. Although the RSM scheme outperforms the proposed scheme with regard to the achieved objective value, it is observed in the simulation results that the solution for RSM does not satisfy the SINR constraints of the CUs with probability 1. *Second*, the performance of the proposed scheme is better than the CPM scheme. Moreover, the performance of CPM scheme first improves with the increase in SINR thresholds and then degrades. The initial improvement results due to rising transmit power requirements for satisfying the SINR constraints. On the other hand, the later degradation is caused by highly directional beamforming toward the CUs to meet the SINR constraints.

The detection probabilities are provided in Fig. 4 for different false alarm rates. The detection performance for the proposed scheme drops with the increase in SINR threshold requirements of CUs. The reason is that meeting a higher SINR requirement of CUs will result in more focused beamforming towards CUs which subsequently degrades the radar detection performance. The detection rate of the CPM scheme can be explained through a similar manner as Fig. 3 results.

Next, we compare the observed SCNR improvement caused by the extra transmit power as compared to the CPM scheme. When the total transmit power for the proposed scheme is equal to the optimal objective value of CPM scheme, then

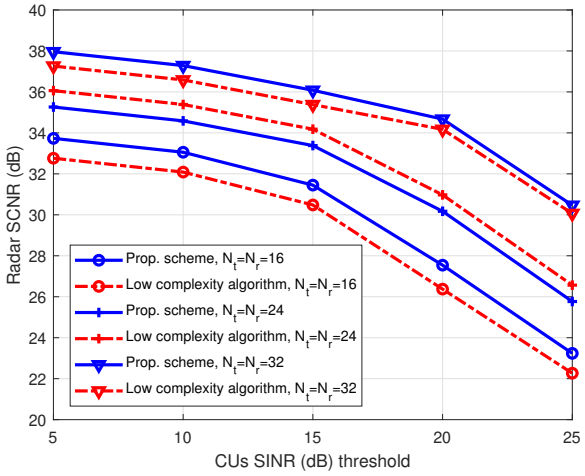

Fig. 6. Comparison between proposed scheme and proposed low complexity scheme.

the SCNR for the proposed scheme and the CPM scheme is same. However, by increasing the available total transmit power, significant improvement in SCNR, such as from 2.5 dB to about 9 dB when $N_t = N_r = 8, \Gamma_k = 4$ dB when the total transmit power is increased by 1 dB to 3 dB as compared to CPM scheme, are observed in Fig. 5. This is due to the fact that the proposed scheme efficiently allocate the extra power in the direction of the target. Thus, improve the EE in the considered ISAC system.

Finally, in Fig. 6, we compare the performance of the proposed and the proposed low complexity schemes. It is observed that the performance of the low complexity scheme is inferior to the proposed scheme. However, the performance gap decreases with the increase in number of antennas. Specially, at higher SINR requirements of CUs, the performance of both proposed schemes is almost identical. Thus, the low complexity scheme is more attractive for the case when more number of antennas are involved, such as millimeter wave or THz communications of 6G, and higher communication QoS is needed.

VII. CONCLUSIONS

This work focuses on beamforming optimization at the DFRC transmitter where the objective was to maximize the radar detection probability while satisfying the communication data rate requirements of CUs. Two scenarios for dealing with the clutter reflections were considered. Although the formulated optimization problems for both scenarios were non-convex, it was shown that global optimality can be achieved for clutter removal scenario and an iterative algorithm was proposed to solve the formulated problem for the scenario where clutter removal was not possible. The optimal solutions were obtained in closed-form, thus reducing the computational complexity of the algorithms. It was also concluded that there is no need to transmit separate probing signal for target detection in both scenarios. Numerical results revealed that the proposed scheme achieves order of magnitude (about 2.5 dB to 9 dB) improvements in terms of radar SCNR as compared to baseline communication power minimization scheme.

APPENDIX

A. Proof of Lemma 1:

Proof. First, we note that **P1-rel** is a convex SDP, and hence the duality gap is zero. Therefore, we consider the Lagrangian of **P1-rel**:

$$\mathcal{L}(\mathbf{U}_k, \mathbf{V}, \eta_k, \omega) = \omega P_{max} + \mathrm{Tr}\left(\sum_{k=1}^{K} \mathbf{U}_k \mathbf{M}_k + \mathbf{T}\mathbf{V}\right) - N_0 \sum_{k=1}^{K} \eta_k, \quad (52)$$

where η_k is the dual variable associated with the k-th SINR constraint, and ω is the dual variable corresponding to the sum power constraint. Furthermore, $\mathbf{M}_k, \mathbf{T}$ are defined as follows:

$$\mathbf{T} = \mathbf{\Phi} - \omega \mathbf{I} - \sum_{k=1}^{K} \eta_k \mathbf{H}_k, \quad (53)$$

and

$$\mathbf{M}_k = \mathbf{\Phi} - \omega \mathbf{I} + \frac{\eta_k}{\Gamma_k} \mathbf{H}_k - \sum_{i=1, i\neq k}^{K} \eta_i \mathbf{H}_i. \quad (54)$$

Hence, the dual problem of **P1-rel** can be written as

$$\begin{aligned} \underset{\omega, \eta_k}{\text{minimize}} \quad & \max_{\mathbf{U}_k, \mathbf{V}} \mathcal{L}\left(\mathbf{U}_k, \mathbf{V}, \eta_k, \omega\right) \\ \text{subject to} \quad & \tilde{C}8: \ \omega \geq 0, \eta_k \geq 0, \end{aligned} \quad (55)$$

with the corresponding optimality conditions given as

$$\mathrm{Tr}(\mathbf{M}_k^* \mathbf{U}_k^*) = 0, \qquad \mathrm{Tr}(\mathbf{T}^* \mathbf{V}^*) = 0, \quad (56)$$

where $\mathbf{M}_k^*, \mathbf{T}^*$ are the corresponding values for η_k^*, ω^*. The problem (55) can be written as

P4:

$$\begin{aligned} \underset{\omega, \eta_k}{\text{minimize}} \quad & \omega P_{max} - N_0 \sum_{k=1}^{K} \eta_k \\ \text{subject to} \quad & \tilde{C}9: \mathbf{M}_k \preceq \mathbf{0}, \mathbf{T} \preceq \mathbf{0}, \omega \geq 0, \eta_k \geq 0. \end{aligned} \quad (57)$$

We have following proposition for **P4** when the optimal values of all the η_k's in **P4** are zero.

Proposition 1. *If none of the $\eta_k > 0$ in the optimal solution of **P4**, then we can set $\mathbf{V}^* = 0, \mathbf{U}_k^* = \frac{P_{max}}{\sum_{i=1}^{K} p_i} p_k \phi \phi^H$ to maximize the objective value of **P1-rel**, where p_k's are obtained from solving the following linear constraints*

$$p_k \,\mathrm{Tr}(\mathbf{H}_k \mathbf{U}_k) \geq \Gamma_k \left(\sum_{i=1, i\neq k}^{K} p_i \,\mathrm{Tr}(\mathbf{H}_k \mathbf{U}_i) + N_0 \right), \quad (58)$$

$$\sum_{k=1}^{K} p_k \leq P_{max}. \quad (59)$$

Proof. First note that when $\eta_k = 0 \ \ \forall \ \ k$, then the optimal value of **P4** is $\zeta_{max} P_{max}$. Now, if we use $\mathbf{V}^* = 0, \mathbf{U}_k^* = \frac{P_{max}}{\sum_{i=1}^{K} p_i} p_k \phi \phi^H$, we will have same objective value for **P1-rel**

and the guarantee to satisfy the rate constraints and sum power are satisfied due to the choice of the values for each p_k through (58), (59). Thus, the proposition is proved. □

Since for the special case of $\eta_k = 0, \quad \forall \quad k$, we have $\text{rank}(\mathbf{U}_k^*) = 1, \text{rank}(\mathbf{V}^*) = 0$, and thus the Lemma 1 is proved for this special case when all the η_k's are zero.

Next, we consider the possibility that there exists a subset $\mathcal{K}$ such that $\eta_{\hat{k}}^* > 0, \forall \quad \hat{k} \in \mathcal{K}$. From (56) and using the fact that $\text{rank}(\mathbf{U}_k^*) \geq 1$ due to the SINR constraints, it can be easily deduced that $\text{rank}(\mathbf{M}_k^*) \leq N_t - 1$. Also, based on $\text{Tr}(\mathbf{T}^*\mathbf{V}^*) = 0$ we have that

$$\eta_{\hat{k}}^* \left(1 + \frac{1}{\Gamma_{\hat{k}}}\right) \text{Tr}(\mathbf{H}_{\hat{k}}\mathbf{V}^*) + \text{Tr}(\mathbf{T}^*\mathbf{V}^*) = \text{Tr}(\mathbf{M}_{\hat{k}}^*\mathbf{V}^*) \leq 0, \quad (60)$$

where the last inequality is a result of the fact that $\mathbf{M}_{\hat{k}}^* \preceq \mathbf{0}$ and $\mathbf{V}^* \succeq \mathbf{0}$. This means $\text{Tr}(\mathbf{H}_{\hat{k}}\mathbf{V}^*) = 0$ which implies

$$\mathbf{H}_{\hat{k}}\mathbf{V}^* = \mathbf{0}, \quad (61)$$

since both $\mathbf{H}_{\hat{k}}, \mathbf{V}^*$ are positive-semidefinite matrices. It follows that

$$(\mathbf{\Phi} - \omega^*\mathbf{I} - \sum_{k \in \mathcal{K}} \eta_k^* \mathbf{H}_k)\mathbf{V}^* = \text{Tr}(\mathbf{T}^*\mathbf{V}^*) = 0, \quad (62)$$

which means $(\mathbf{\Phi} - \omega^*\mathbf{I})\mathbf{V}^* = \mathbf{0}$. Thus, $\mathbf{V}^*$ must be orthogonal to $\mathbf{H}_k$ as well as $(\mathbf{\Phi} - \omega^*\mathbf{I})$. In what follows, we make use of the following identities about the rank of matrices

$$\text{rank}(\mathbf{AB}) \leq \min(\text{rank}(\mathbf{A}), \text{rank}(\mathbf{B})), \quad (63)$$

$$\text{rank}(-\mathbf{A}) = \text{rank}(\mathbf{A}). \quad (64)$$

Then, it can be established that $\text{rank}(\mathbf{\Phi}) = 1, \text{rank}(\mathbf{H}_k) = 1, \text{rank}(\mathbf{\Phi} - \omega^*\mathbf{I}) \geq N_t - 1$. Since we have assumed that $\mathbf{H}_k$ and $\mathbf{\Phi}$ are independent, the combined dimensions of $\mathbf{\Phi} - \omega^*\mathbf{I}$, $\mathbf{H}_k$ are N_t. Hence, we conclude that $\mathbf{V}^* = \mathbf{0}$ since it is orthogonal to the total number of dimensions N_t. Hence, the second property in the Lemma 1 is proved for all possible cases.

To prove the first property in Lemma 1, we note that in order to satisfy (56), $\mathbf{V}^*$ must be a zero matrix. Therefore, $\mathbf{T}^*$ must be full rank, i.e. $\text{rank}(\mathbf{T}^*) = N_t$. Also, we have

$$\mathbf{T}^* = \mathbf{M}_k^* - \eta_k^* \left(1 + \frac{1}{\Gamma_k}\right) \mathbf{H}_k. \quad (65)$$

Multiplying $\mathbf{U}_k^*$ on both sides of (70) and using (61) we get

$$\mathbf{T}^*\mathbf{U}_k^* = -\eta_k^* \left(1 + \frac{1}{\Gamma_k}\right) \mathbf{H}_k\mathbf{U}_k^*, \quad (66)$$

and since $\mathbf{T}^*$ is full rank, we must have $\text{rank}(\mathbf{T}^*\mathbf{U}_k^*) = \text{rank}(\mathbf{U}_k^*)$ and hence from (66) we have

$$\text{rank}(\mathbf{U}_k^*) = \text{rank}\left(-\eta_k^* \left(1 + \frac{1}{\Gamma_k}\right) \mathbf{H}_k\mathbf{U}_k^*\right) \leq 1, \quad (67)$$

where we have used (68), (69) and the fact that $\text{rank}(\mathbf{H}_k) = 1$. Combining (67) with the earlier observation that $\text{rank}(\mathbf{U}_k^*) \geq 1$ to satisfy the SINR constraint of k-th CU, we conclude $\text{rank}(\mathbf{U}_k^*) = 1$. This completes the proof of the first property in Lemma 1. □

B. Proof of Lemma 2:

Proof. Let us denote the optimal value of **P1** as x^* and that of **P1-d** as y^*. It is clear that $y^* \geq x^*$ due to the fact that the optimal value of the dual of a maximization problem provides an upper bound to the optimal value the problem.

In order to show that $y^* \leq x^*$, note that the duality gap between SDR of **P1**, denoted as **SDRP1** with optimal value x_{SDRP1}^*, and its dual, denoted as **SDRP1D** with optimal value y_{SDRP1D}^*, is zero since its a convex optimization problem and the Slater conditions [42] are satisfied. Hence, we must have $x_{SDRP1}^* = y_{SDRP1D}^* \geq y^*$. Also from Lemma 1, we have that SDR relaxation of **P1** is tight i.e. $x^* = x_{SDRP1}^*$. Therefore, we conclude that $x^* \geq y^*$. This completes the proof. □

C. Proof of Lemma 3

Proof. We note that if $\mathbf{u}_k$ is an optimal solution, then $\mathbf{u}_k^* e^{j\theta_k}$ is also an optimal solution since it does not violate any constraints of **P1** and achieves the same objective value. This means we can apply any phase rotation to $\mathbf{u}_k$ to make sure that $\mathbf{h}_k^H\mathbf{u}_k$ is a real positive value. □

D. Proof of Lemma 4

Proof. Taking the derivative of (25) and putting it equal to zero, we get

$$\mathbf{u}_k = \left[\omega\mathbf{I} - \mathbf{\Phi} + \sum_{i=1, i\neq k}^{K} \eta_i \mathbf{h}_i\mathbf{h}_i^H\right]^{-1} \eta_k \mathbf{h}_k\mathbf{h}_k^H\mathbf{u}_k. \quad (68)$$

Now according to Lemma 3, without loss of generality $\mathbf{h}_k^H\mathbf{u}_k$ is a positive scalar value. Therefore, the optimal value of $\mathbf{u}_k$ is parallel to $\left[\omega\mathbf{I} - \mathbf{\Phi} + \sum_{i=1, i\neq k}^{K} \eta_i \mathbf{h}_i\mathbf{h}_i^H\right]^{-1} \mathbf{h}_k$ since $\eta_k \geq 0$. Hence, we have

$$\mathbf{u}_k = \sqrt{p_k} \frac{\left[\omega\mathbf{I} - \mathbf{\Phi} + \sum_{i=1, i\neq k}^{K} \eta_i \mathbf{h}_i\mathbf{h}_i^H\right]^{-1} \mathbf{h}_k}{\left\|\left[\omega\mathbf{I} - \mathbf{\Phi} + \sum_{i=1, i\neq k}^{K} \eta_i \mathbf{h}_i\mathbf{h}_i^H\right]^{-1} \mathbf{h}_k\right\|}. \quad (69)$$

Hence, (27) is proved. In order to find the values of $\{p_k\}$, first we note that none of the values η_k is zero and all of the η_k's are bounded from above. This statement can be proved with the help of (68) as follows. From (68) we can conclude

$$\eta_k = \frac{N_0\Gamma_k}{\mathbf{h}_k^H \left(\omega I - \mathbf{\Phi} + \sum_{i=1, i\neq k}^{K} \eta_i \mathbf{h}_i\mathbf{h}_i^H\right)^{-1} \mathbf{h}_k}. \quad (70)$$

Now recall from the discussion in the proof of Lemma 1 that $\text{rank}(\omega\mathbf{I} - \mathbf{\Phi}) \geq N_t - 1$ and since $\mathbf{h}_k$'s and steering vectors are independent, $\omega\mathbf{I} - \mathbf{\Phi} + \sum_{i=1, i\neq k}^{K} \eta_i \mathbf{h}_i\mathbf{h}_i^H$ is a full rank positive definite matrix. Therefore, from (70) we have $\eta_k > 0$ and these values are bounded from above. Using this observation, and the existence of zero duality gap, it is easy to see that the SINR constraints must be met with equality

$$\Gamma_k \sum_{i=1, i\neq k}^{K} |\mathbf{h}_k^H\mathbf{u}_i|^2 + \Gamma_k N_o = |\mathbf{h_k}^H\mathbf{u}_k|^2. \quad (71)$$

From (71) we can obtain the values for $\{p_k\}$ and the proof is completed. □

E. Proof of Lemma 5

Proof. First we assume that the optimal solution for the dual problem of **P2'-SDR** has all $\eta_k^* = 0$, where η_k^* is the optimal dual variable corresponding to the k-th SINR constraint. Then, we can use an argument similar to Proposition 1 to show that we can obtain a new optimal solution where $\mathbf{V}^* = \mathbf{0}$ and $\mathbf{U}_k^* = \frac{P_{max}p_k'}{\sum_{i=1}^K p_i'}\phi'\phi'^H$ where ϕ' is the eigenvector corresponding to the largest eigenvalue of $\mathbf{\Phi}'$. Moreover, p_k' are the solution to the following linear inequalities

$$p_k' \operatorname{Tr}(\mathbf{H}_k\mathbf{U}_k) \geq \Gamma_k \left(\sum_{i=1, i\neq k}^{K} p_i' \operatorname{Tr}(\mathbf{H}_k\mathbf{U}_i) + N_0 \right), \quad (72)$$

$$\sum_{k=1}^{K} p_k' \leq P_{max}. \quad (73)$$

Hence, the proof is complete for the special case when $\eta_k^* = 0$, $\forall k \in \{1, \cdots, K\}$. Next, we consider the possibility that at least one of $\eta_k^* \neq 0$. To prove that $\mathbf{V}^* = \mathbf{0}$, assume that the optimal solution to **P2'-SDR** is $\{\mathbf{U}_k^*\}$, and $\mathbf{V}^* \neq \mathbf{0}$. Then, we can obtain another solution $\{\mathbf{U}'^*_k\}, \mathbf{V}'^* = \mathbf{0}$ of **P2'-SDR** such that $\mathbf{U}'^*_{\hat{k}} = \mathbf{U}_k^* + \mathbf{V}^*$ for some $k \in \{1, \cdots, K\}$, $\mathbf{U}'^*_k = \mathbf{U}_k^*, \forall k \in \{1, \cdots, K\} \setminus \hat{k}$ and $\mathbf{V}'^* = \mathbf{0}$. By doing so, we can easily observe that the optimal value for the modified solution $\{\mathbf{U}'^*_k\}, \mathbf{V}'^* = \mathbf{0}$ is exactly the same as that achieved by $\{\mathbf{U}_k^*\}, \mathbf{V}^* \neq \mathbf{0}$. Furthermore, it is easy to verify that all the constraints in **P2'-SDR** are satisfied for the modified solution. This proves the first statement of Lemma 5 for the case when at least one of η_k' is positive. In order to proceed further, we set $\mathbf{V} = \mathbf{0}$ in **P2'-SDR**. Then **P2'-SDR** can be written as

P2'-SDR:

$$\begin{aligned} \underset{\mathbf{U}_k}{\text{maximize}} \quad & \sum_{k=1}^{K} \operatorname{Tr}(\mathbf{\Phi}'\mathbf{U}_k) \\ \text{subject to} \quad & \tilde{C}1 - \tilde{C}3. \end{aligned} \quad (74)$$

Using a well known result in [43, Theorem 3.2], it can be shown that there exist rank one solutions for all $\mathbf{U}_k$'s for **P2'-SDR**. □

F. Proof of Lemma 6

Proof. In order to prove this lemma, first we note that the sum of Toeplitz matrices is also a Toeplitz matrix. Also, $\mathbf{I}$ is a Toeplitz matrix. We only need to show that $\mathbf{A}(\theta_i)\mathbf{u}_k\mathbf{u}_k^H\mathbf{A}^H(\theta_i)$ is a Toeplitz matrix for each $i \in \{1, \cdots, I\}$ and $k \in \{1, \cdots, K\}$. Note that

$$\mathbf{A}(\theta_i)\mathbf{u}_k\mathbf{u}_k^H\mathbf{A}^H(\theta_i) = \underbrace{|\mathbf{a}_t^H(\theta_i)\mathbf{u}_k|^2}_{\text{positive scalar}} \mathbf{a}_r(\theta_i)\mathbf{a}_r^H(\theta_i), \quad (75)$$

where we have used the definition of $\mathbf{A}(\theta) = \mathbf{a}_r(\theta)\mathbf{a}_t^H(\theta)$. Furthermore, note that $\mathbf{a}_r(\theta)\mathbf{a}_r^H(\theta)$ has following form

$$\mathbf{\Xi}(\theta_i) = \begin{bmatrix} 1 & z_i & z_i^2 & \cdots & z_i^{N_r-1} \\ z_i^{-1} & 1 & z_i & \ddots & \vdots \\ z_i^{-2} & z_i^{-1} & 1 & \ddots & z_i^2 \\ \vdots & \ddots & \ddots & \ddots & z_i \\ z_i^{-(N_r-1)} & \cdots & z_i^{-2} & z_i^{-1} & 1 \end{bmatrix}, \quad (76)$$

where $z_i^m = e^{-j\pi m\lambda \sin(\theta_i)}, \forall\ m \in \{0, \cdots, N_r - 1\}$. Since $\mathbf{\Xi}(\theta_i)$ follows the general Toeplitz structure, $\mathbf{S}$, hence $\mathbf{\Xi}(\theta_i)$ is a Toeplitz matrix. Combining this fact with the additive property of Toeplitz matrices, we conclude that $\mathbf{W}(\{\mathbf{u}_k\})$ is a Toeplitz matrix. □

G. Proof of Lemma 7

Proof. This lemma follows from the fact that any Hermitian Circulant matrix has a eigenvalue decomposition where the eigenvectors are the columns of discrete Fourier transform (DFT) matrix. Hence, we can write $\mathbf{X}^{-1} = \left(\mathbf{F}^H\mathbf{D}\mathbf{F}\right)^{-1} = \mathbf{F}^H$, where $\mathbf{D}$ is the diagonal matrix whose diagonal elements are the eigenvalues of $\mathbf{X}$. Thus, we have $\mathbf{X}^{-1} = \mathbf{F}^H\mathbf{D}^{-1}\mathbf{F}$. □

H. Proof of Lemma 8

Proof. In order to proof this lemma, first we show that

$$\mathbf{u}_k^H\mathbf{A}^H(\theta_0)\mathbf{W}^{-1}\mathbf{A}(\theta_0)\mathbf{u}_k \simeq \mathbf{u}_k^H\mathbf{A}^H(\theta_0)\mathbf{G}^{-1}\mathbf{A}(\theta_0)\mathbf{u}_k, \quad (77)$$

where $\mathbf{G}$ denotes the Circulant matrix approximation of $\mathbf{W}$ and $\mathbf{\Lambda}$ is a diagonal matrix in which the diagonal elements are the eigenvalues of matrix $\mathbf{G}$. Then, we extend this result over the summation for $k \in \{1, \cdots, K\}$ by noting the inequality $\sum_{k=1}^K y_k \leq \sum_{k=1}^K |y_k|$. Hence, we need to show that

$$\begin{aligned} \lim_{N_r\to\infty} \Bigg| & \operatorname{Tr}\left(\mathbf{A}(\theta_0)\mathbf{u}_k\mathbf{u}_k^H\mathbf{A}^H(\theta_0)\mathbf{W}^{-1}\right) \\ & - \operatorname{Tr}\left(\mathbf{A}(\theta_0)\mathbf{u}_k\mathbf{u}_k^H\mathbf{A}^H(\theta_0)\mathbf{G}^{-1}\right)\Bigg| \leq 0. \end{aligned} \quad (78)$$

Toward this end, we use the matrix trace inequality to get

$$\begin{aligned} \Big| \operatorname{Tr}\left(\mathbf{A}(\theta_0)\mathbf{u}_k\mathbf{u}_k^H\mathbf{A}^H(\theta_0)\ \mathbf{W}^{-1}\right) - \operatorname{Tr}\left(\mathbf{A}(\theta_0)\mathbf{u}_k\mathbf{u}_k^H\mathbf{A}^H(\theta_0)\mathbf{G}^{-1}\right)\Big| \\ \leq \operatorname{Tr}\left(\mathbf{\Phi_k}\right) \operatorname{Tr}\left(\mathbf{W}^{-1} - \mathbf{G}^{-1}\right), \end{aligned} \quad (79)$$

where $\mathbf{\Phi_k} = \mathbf{A}(\theta_0)\mathbf{u}_k\mathbf{u}_k^H\mathbf{A}^H(\theta_0)$. Also, from the maximum power constraint we have

$$\operatorname{Tr}\left(\mathbf{\Phi}_k\right) \leq P_{max}. \quad (80)$$

Therefore, the inequality (79) can be written as

$$\begin{aligned} \Big| \operatorname{Tr}\left(\mathbf{A}(\theta_0)\mathbf{u}_k\mathbf{u}_k^H\mathbf{A}^H(\theta_0)\ \mathbf{W}^{-1}\right) - \operatorname{Tr}\left(\mathbf{A}(\theta_0)\mathbf{u}_k\mathbf{u}_k^H\mathbf{A}^H(\theta_0)\mathbf{G}^{-1}\right)\Big| \\ \leq P_{max} \operatorname{Tr}\left(\mathbf{W}^{-1} - \mathbf{G}^{-1}\right). \end{aligned} \quad (81)$$

Assume that n-th eigenvalue of $\mathbf{W}$ and $\mathbf{G}$ are denoted by $c_{min} \leq \tau_n \leq c_{max}$ and $c_{min} \leq \iota_n \leq c_{max}$, respectively. Then, we have

$$\begin{aligned} \operatorname{Tr}\left(\mathbf{W}^{-1} - \mathbf{G}^{-1}\right) &= \operatorname{Tr}\left(\mathbf{W}^{-1}\right) - \operatorname{Tr}(\mathbf{G}^{-1}) \\ &= \frac{1}{c_{max}} \left(\sum_{n=1}^{N_r} \frac{1}{\hat{\tau}_n} - \sum_{n=1}^{N_r} \frac{1}{\hat{\iota}_n} \right), \end{aligned} \quad (82)$$

where $\hat{\tau}_n = \frac{\tau_n}{c_{max}}$ and $\hat{\iota}_n = \frac{\iota_n}{c_{max}}$. After simplifications, we can write the right hand side (RHS) of (82) as

$$\sum_{n=1}^{N_r} \frac{1}{\hat{\tau}_n} - \sum_{n=1}^{N_r} \frac{1}{\hat{\iota}_n} = \frac{\left(\prod_{n=1}^{N_r} \hat{\iota}_n\right)\left(\sum_{j=1}^{N_r} \prod_{l=1, l\neq j}^{N_r} \hat{\tau}_l\right)}{\left(\prod_{n=1}^{N_r} \hat{\iota}_n\right)\left(\prod_{n=1}^{N_r} \hat{\tau}_n\right)}$$

$$-\frac{\left(\prod_{n=1}^{N_r}\hat{\tau}_n\right)\left(\sum_{j=1}^{N_r}\prod_{l=1,l\neq j}^{N_r}\hat{\iota}_l\right)}{\left(\prod_{n=1}^{N_r}\hat{\iota}_n\right)\left(\prod_{n=1}^{N_r}\hat{\tau}_n\right)}. \quad (83)$$

Next, without loss of generality[1], we assume $\prod_{n=1}^{N_r}\hat{\tau}_n \geq \prod_{n=1}^{N_r}\hat{\iota}_n$ then we can derive the following upper bound on (83)

$$\sum_{n=1}^{N_r}\frac{1}{\hat{\tau}_n}-\sum_{n=1}^{N_r}\frac{1}{\hat{\iota}_n} \leq \frac{\sum_{j=1}^{N_r}\prod_{l=1,l\neq j}^{N_r}\hat{\tau}_l-\sum_{j=1}^{N_r}\prod_{l=1,l\neq j}^{N_r}\hat{\iota}_l}{\prod_{n=1}^{N_r}\hat{\iota}_n} \leq \frac{\left|\sum_{j=1}^{N_r}\prod_{l=1,l\neq j}^{N_r}\hat{\tau}_l-\sum_{j=1}^{N_r}\prod_{l=1,l\neq j}^{N_r}\hat{\iota}_l\right|}{\prod_{n=1}^{N_r}\hat{\iota}_n}. \quad (84)$$

Furthermore, using the Triangle inequality on the RHS of (84), we can write

$$\sum_{n=1}^{N_r}\frac{1}{\hat{\tau}_n}-\sum_{n=1}^{N_r}\frac{1}{\hat{\iota}_n} \leq \sum_{j=1}^{N_r}\frac{\left|\prod_{l=1,l\neq j}^{N_r}\hat{\tau}_l-\prod_{l=1,l\neq j}^{N_r}\hat{\iota}_l\right|}{\prod_{n=1}^{N_r}\hat{\iota}_n}. \quad (85)$$

Before proceeding further, we note that

$$|t_1t_2-s_1s_2| \leq |t_1-s_1|+|t_2-s_2|, \quad (86)$$

for all $|t_1| \leq 1, |s_1| \leq 1, |t_2| \leq 1, |s_2| \leq 1$, which can be expanded to

$$\left|\prod_{n=1}^{N}t_n-\prod_{n=1}^{N}s_n\right| \leq \sum_{n=1}^{N}|t_n-s_n|, \quad \forall \ \ |t_n| \leq 1, |s_n| \leq 1, \quad (87)$$

for all $n \ \in \{1,\cdots,N\}$ by induction. Consider a single term on the RHS of (85) for $j=1$. Then, with the help of (87), we can write

$$\frac{\left|\prod_{l=1,l\neq 1}^{N_r}\hat{\tau}_l-\prod_{l=1,l\neq 1}^{N_r}\hat{\iota}_l\right|}{\prod_{n=1}^{N_r}\hat{\iota}_n} \leq \frac{\sum_{l=2}^{N_r}|\hat{\tau}_l-\hat{\iota}_l|}{\prod_{n=1}^{N_r}\hat{\iota}_n} \leq \frac{\sum_{l=1}^{N_r}|\tau_l-\iota_l|}{c_{max}\det(\mathbf{G})} \quad (88)$$

where $\det(\mathbf{G})$ denote the determinant of the matrix $\mathbf{G}$. Next, using the following result about the Circulant matrix approximation of Teoplitz matrix from [44, Theorem 1]

$$\lim_{N_r\to\infty}\max_{n\in\{1,2,\cdots,N_t\}}|\tau_n-\iota_n|=0, \quad (89)$$

we can write

$$\lim_{N_r\to\infty}\frac{\left|\prod_{l=1,l\neq 1}^{N_r}\hat{\tau}_l-\prod_{l=1,l\neq 1}^{N_r}\hat{\iota}_l\right|}{\prod_{n=1}^{N_r}\hat{\iota}_n} \leq 0. \quad (90)$$

The result in (90) can be obtained for all the terms on the RHS of (85). Thus, we have

$$\lim_{N_r\to\infty}\sum_{n=1}^{N_r}\frac{1}{\hat{\tau}_n}-\sum_{n=1}^{N_r}\frac{1}{\hat{\iota}_n} \leq 0. \quad (91)$$

Combining the result in (91) with (82) and (81), we get (92), shown at the top of next page. Finally, summing (92) over all $k \in \{1,2,\cdots,K\}$ we get (93), (94). This completes the proof. □

[1]Note that, the procedure can also be applied for the other case, since we are using the absolute values in our proof subsequently. Hence, we consider only one case to save space.

REFERENCES

[1] T. L. Ericsson. (2021) Mobile data traffic outlook. [Online]. Available: https://www.ericsson.com/en/reports-and-papers/mobility-report/dataforecasts/mobile-traffic-forecast.

[2] G. Fagas, J. P. Gallagher, L. Gammaitoni, and D. J. Paul, "Energy challenges for ICT," in *ICT - Energy Concepts for Energy Efficiency and Sustainability*. Rijeka: IntechOpen, 2017, ch. 1. [Online]. Available: https://doi.org/10.5772/66678.

[3] A. S. G. Andrae and T. Edler, "On global electricity usage of communication technology: Trends to 2030," *Challenges*, vol. 6, no. 1, pp. 117–157, 2015. [Online]. Available: https://www.mdpi.com/2078-1547/6/1/117.

[4] X. Y. Zhou, W. S. Chan, S. Chen, and W. J. Feng, "Broadband highly efficient Doherty power amplifiers," *IEEE Cir. Sys. Mag.*, vol. 20, no. 4, pp. 47–64, 2020.

[5] E. S. Li, C.-T. Lin, H. Jin, and K.-S. Chin, "A broadband balun with complex impedance transformation and high isolation," *IEEE Access*, vol. 7, pp. 112 295–112 303, 2019.

[6] R. Kumar, R. Singh, and R. K. Chaudhary, "Miniaturised triple-band antenna loaded with complementary concentric closed ring resonators with asymmetric coplanar waveguide-fed based on epsilon negative transmission line," *IET Micr., Ant. & Prop.*, vol. 12, no. 13, pp. 2073–2079, 2018.

[7] P. P. Campo, L. Anttila, V. Lampu, M. Allén, Y. Guo, N. Wang, and M. Valkama, "Inverse covariance matrix estimation for low-complexity closed-loop DPD systems: Methods and performance," *IEEE Trans Mic. Theory Tech.*, vol. 70, no. 3, pp. 1474–1489, Mar. 2022.

[8] S. Wang, M. Roger, J. Sarrazin, and C. Lelandais-Perrault, "Augmented iterative learning control for neural-network-based joint crest factor reduction and digital predistortion of power amplifiers," *IEEE Trans. Micr. Theory and Tech.*, vol. 68, no. 11, pp. 4835–4845, Nov. 2020.

[9] L. Zhao, M. Li, C. Liu, S. V. Hanly, I. B. Collings, and P. A. Whiting, "Energy efficient hybrid beamforming for multi-user millimeter wave communication with low-resolution A/D at transceivers," *IEEE J. Sel. Areas Comm.*, vol. 38, no. 9, pp. 2142–2155, Sep. 2020.

[10] A. Zhang, M. L. Rahman, X. Huang, Y. J. Guo, S. Chen, and R. W. Heath, "Perceptive mobile networks: Cellular networks with radio vision via joint communication and radar sensing," *IEEE Vehi. Tech. Mag.*, vol. 16, no. 2, pp. 20–30, Jun. 2021.

[11] L. Zheng, M. Lops, Y. C. Eldar, and X. Wang, "Radar and communication coexistence: An overview: A review of recent methods," *IEEE Sig. Proc. Mag.*, vol. 36, no. 5, pp. 85–99, Sep. 2019.

[12] E. Dahlman, S. Parkvall, and J. Sköld, "Chapter 8 - Channel sounding," in *5G NR (Second Edition)*, second edition ed. Academic Press, 2021, pp. 147–164. [Online]. Available: https://www.sciencedirect.com/science/article/pii/B9780128223208000088.

[13] B. Sun, B. Tan, W. Wang, and E. S. Lohan, "A comparative study of 3D UE positioning in 5G new radio with a single station," *Sensors*, vol. 21, no. 4, 2021. [Online]. Available: https://www.mdpi.com/1424-8220/21/4/1178.

[14] B. Sun, B. Tan, W. Wang, M. Valkama, and E. S. Lohan, "Embedding the radio imaging in 5G networks: Signal processing and an airport use case," in *2021 IEEE 94th Vehicular Technology Conference (VTC2021-Fall)*, 2021, pp. 01–05.

[15] F. Dong, F. Liu, Y. Cui, W. Wang, K. Han, and Z. Wang, "Sensing as a service in 6G perceptive networks: A unified framework for ISAC resource allocation," *arXiv:2202.09969*, 2022.

[16] HBR, "5G Frequency Bands," https://halberdbastion.com/technology/cellular/5g-nr/5g-frequency-bands, accessed: 2022-9-21.

[17] H. Tataria, M. Shafi, A. F. Molisch, M. Dohler, H. Sjöland, and F. Tufvesson, "6G wireless systems: Vision, requirements, challenges, insights, and opportunities," *Proceedings of the IEEE*, vol. 109, no. 7, pp. 1166–1199, 2021.

[18] C. Chaccour, M. N. Soorki, W. Saad, M. Bennis, P. Popovski, and M. Debbah, "Seven defining features of Terahertz (THz) wireless systems: A fellowship of communication and sensing," *IEEE Commun. Sur. Tut.*, vol. 24, no. 2, pp. 967–993, 2022.

[19] H. Sarieddeen, N. Saeed, T. Y. Al-Naffouri, and M.-S. Alouini, "Next generation Terahertz communications: A rendezvous of sensing, imaging, and localization," *IEEE Commun. Mag.*, vol. 58, no. 5, pp. 69–75, May 2020.

[20] C. Chaccour, W. Saad, O. Semiari, M. Bennis, and P. Popovski, "Joint sensing and communication for situational awareness in wireless thz systems," in *ICC 2022 - IEEE International Conference on Communications*, 2022, pp. 3772–3777.

$$\lim_{N_r\to\infty}\left|\left(\mathrm{Tr}\left(\mathbf{A}(\theta_0)\mathbf{u}_k\mathbf{u}_k^H\mathbf{A}^H(\theta_0)\mathbf{W}^{-1}\right)-\mathrm{Tr}\left(\mathbf{A}(\theta_0)\mathbf{u}_k\mathbf{u}_k^H\mathbf{A}^H(\theta_0)\mathbf{G}^{-1}\right)\right)\right|\leq 0. \tag{92}$$

$$\lim_{N_r\to\infty}|\alpha_0|^2\sum_{k=1}^{K}\mathbf{u}_k^H\boldsymbol{\Phi}'\mathbf{u}_k-|\alpha_0|^2\sum_{k=1}^{K}\tilde{\mathbf{u}}_k^H\tilde{\boldsymbol{\Lambda}}\tilde{\mathbf{u}}_k\leq\lim_{N_r\to\infty}|\alpha_0|^2\left|\sum_{k=1}^{K}\mathbf{u}_k^H\boldsymbol{\Phi}'\mathbf{u}_k-\sum_{k=1}^{K}\tilde{\mathbf{u}}_k^H\tilde{\boldsymbol{\Lambda}}\tilde{\mathbf{u}}_k\right| \tag{93}$$

$$\leq|\alpha_0|^2\sum_{k=1}^{K}\lim_{N_r\to\infty}\left|\mathbf{u}_k^H\boldsymbol{\Phi}'_k\mathbf{u}_k-\tilde{\mathbf{u}}_k^H\tilde{\boldsymbol{\Lambda}}\tilde{\mathbf{u}}_k\right|\leq 0. \tag{94}$$

[21] "P.1410: Propagation data and prediction methods required for the design of terrestrial broadband radio access systems operating in a frequency range from 3 to 60 GHz," ITU-R Technical recommendation, 2012.

[22] 3GPP, "Study on channel model for frequencies from 0.5 to 100 GHz (Release 14)," 3GPP TR 38.901 V14.1.1, July 2017.

[23] T. Bai and R. W. Heath, "Coverage and rate analysis for millimeter-wave cellular networks," *IEEE Trans. Wirel. Comm.*, vol. 14, no. 2, pp. 1100–1114, Feb. 2014.

[24] M. Gapeyenko, A. Samuylov, M. Gerasimenko, D. Moltchanov, S. Singh, M. R. Akdeniz, E. Aryafar, N. Himayat, S. Andreev, and Y. Koucheryavy, "On the temporal effects of mobile blockers in urban millimeter-wave cellular scenarios," *IEEE Trans. Veh. Techn.*, vol. 66, no. 11, pp. 10 124–10 138, Nov. 2017.

[25] C. D. Ozkaptan, E. Ekici, and O. Altintas, "Adaptive waveform design for communication-enabled automotive radars," *IEEE Trans. Wirel. Comm.*, vol. 21, no. 6, pp. 3965–3978, Jun. 2022.

[26] P. Kumari, N. J. Myers, and R. W. Heath, "Adaptive and fast combined waveform-beamforming design for MMWave automotive joint communication-radar," *IEEE J. Sel. Top. Sig. Proc.*, vol. 15, no. 4, pp. 996–1012, Jun. 2021.

[27] J. A. Zhang, F. Liu, C. Masouros, R. W. Heath, Z. Feng, L. Zheng, and A. Petropulu, "An overview of signal processing techniques for joint communication and radar sensing," *IEEE J. Sel. Top. Sig. Proc.*, vol. 15, no. 6, pp. 1295–1315, Nov. 2021.

[28] S. Xu, L. Wu, K. Doğançay, and M. Alaee-Kerahroodi, "A hybrid approach to optimal TOA-sensor placement with fixed shared sensors for simultaneous multi-target localization," *IEEE Trans. Sig. Proc.*, vol. 70, pp. 1197–1212, 2022.

[29] Y. Rong, A. Aubry, A. De Maio, and M. Tang, "Adaptive radar detection in Gaussian interference using clutter-free training data," *IEEE Trans. Sig. Proc.*, vol. 70, pp. 978–993, 2022.

[30] F. Liu, Y.-F. Liu, A. Li, C. Masouros, and Y. C. Eldar, "Cramér-Rao bound optimization for joint radar-communication beamforming," *IEEE Trans. Sig. Proc.*, vol. 70, pp. 240–253, 2022.

[31] I. Valiulahi, C. Masouros, A. Salem, and F. Liu, "Antenna selection for energy-efficient dual-functional radar-communication systems," *IEEE Wirel. Comm. Lett.*, vol. 11, no. 4, pp. 741–745, Apr. 2022.

[32] X. Li, F. Liu, Z. Zhou, G. Zhu, S. Wang, K. Huang, and Y. Gong, "Integrated sensing, communication, and computation over-the-Aair: MIMO beamforming design," *arXiv:2201.12581*, 2022.

[33] A. De Maio, S. De Nicola, Y. Huang, Z.-Q. Luo, and S. Zhang, "Design of phase codes for radar performance optimization with a similarity constraint," *IEEE Trans. Sig. Proc.*, vol. 57, no. 2, pp. 610–621, Feb. 2009.

[34] G. Cui, H. Li, and M. Rangaswamy, "MIMO radar waveform design with constant modulus and similarity constraints," *IEEE Trans. Sig. Proc.*, vol. 62, no. 2, pp. 343–353, Feb. 2014.

[35] O. Aldayel, V. Monga, and M. Rangaswamy, "Successive QCQP refinement for MIMO radar waveform design under practical constraints," *IEEE Trans. Sig. Proc.*, vol. 64, no. 14, pp. 3760–3774, 2016.

[36] G. Cui, X. Yu, V. Carotenuto, and L. Kong, "Space-time transmit code and receive filter design for colocated MIMO radar," *IEEE Trans. Sig. Proc.*, vol. 65, no. 5, pp. 1116–1129, 2017.

[37] L. Wu, P. Babu, and D. P. Palomar, "Transmit waveform/receive filter design for MIMO radar with multiple waveform constraints," *IEEE Trans. Sig. Proc.*, vol. 66, no. 6, pp. 1526–1540, Jun. 2018.

[38] L. Chen, F. Liu, J. Liu, and C. Masouros, "Composite signalling for DFRC: Dedicated probing signal or not?" *arXiv:2009.03528*, 2020.

[39] T. Guo and R. Qiu, "OFDM waveform design compromising spectral nulling, side-lobe suppression and range resolution," in *2014 IEEE Radar Conference*, 2014, pp. 1424–1429.

[40] Z.-q. Luo, W.-k. Ma, A. M.-c. So, Y. Ye, and S. Zhang, "Semidefinite relaxation of Quadratic optimization problems," *IEEE Sig. Proc. Mag.*, vol. 27, no. 3, pp. 20–34, May 2010.

[41] E. Björnson, M. Bengtsson, and B. Ottersten, "Optimal multiuser transmit beamforming: A difficult problem with a simple solution structure [lecture notes]," *IEEE Sig. Proc. Mag.*, vol. 31, no. 4, pp. 142–148, Jul. 2014.

[42] S. Boyd and L. Vandenberghe, *Convex optimization*. Cambridge university press, 2004.

[43] Y. Huang and D. P. Palomar, "Rank-constrained separable semidefinite programming with applications to optimal beamforming," *IEEE Trans. Sig. Proc.*, vol. 58, no. 2, pp. 664–678, Feb. 2010.

[44] Z. Zhu and M. B. Wakin, "On the asymptotic equivalence of circulant and toeplitz matrices," *IEEE Trans. Inf. Theory*, vol. 63, no. 5, pp. 2975–2992, May 2017.

Mateen Ashraf received PhD in wireless communication engineering in 2017. He is currently working as a research fellow in Tampere University. His current research interest includes beamforming design for integrated sensing and communication (ISAC) systems for 6G networks and intelligent reflection surface assisted wireless energy harvesting systems. He has published several journal and conference paper in leading IEEE journals and conferences. He is an active reviewer of many leading journals and has acted as TPC member for prestigious IEEE conferences.

Dr Bo Tan received his PhD in digital communications from the University of Edinburgh, UK, in Nov 2013, then carried out postdoc research at University College London and the University of Bristol, UK, on radio sensing solutions for healthcare, robotics and security applications. He has been a tenure track Assistant Professor at Tampere University, Finland, since 2019. His current research focuses on integrating connectivity and sensing for intelligent machines. He is the PI of multiple Academic of Finland, Business Finland and Horizon European MSCA projects. He is the reviewer of IEEE/IET/ACM journals on radar, wireless communications and pervasive sensing/computing.

Dmitri Moltchanov received the M.Sc. and Cand.Sc. degrees from the St. Petersburg State University of Telecommunications, Russia, in 2000 and 2003, respectively, and the Ph.D. degree from the Tampere University of Technology in 2006. Currently he is University Lecturer in with the Laboratory of Electronics and Communications Engineering, Tampere University, Finland. He has (co-)authored over 200 publications on wireless communications, heterogeneous networking, IoT applications, applied queuing theory. In his career he has taught more than 50 full courses on wireless and wired networking technologies, P2P/IoT systems, network modeling, queuing theory, etc. His current research interests include research and development of 5G+/6G systems, ultra-reliable low-latency service, industrial IoT applications, and mission-critical V2V/V2X systems.

John S. Thompson (Fellow, IEEE) received the Ph.D. degree in electrical engineering from The University of Edinburgh, Edinburgh, U.K., in 1996, where he currently holds a Personal Chair of Signal Processing and Communications with the School of Engineering. He specializes in antenna array processing, energy-efficient wireless communications, and the application of machine learning to wireless communications problems. To date, he has published in excess of 350 papers on these topics. His work has been regularly cited by the wireless community and from 2015 to 2018, he was recognized by Thomson Reuters as a Highly Cited Researcher. He is currently an Area Editor handling wireless communications topics for the IEEE TRANSACTIONS ON GREEN COMMUNICATIONS AND NETWORKING. In January 2016, he was elevated to Fellow of the IEEE for Contributions to Antenna Arrays and Multihop Communications.

Mikko Valkama [S'00, M'01, SM'15, F'22] received his M.Sc. (Tech.) and D.Sc. (Tech.) degrees (both with honors) from Tampere University of Technology, Finland, in 2000 and 2001, respectively. In 2003, he was with the Communications Systems and Signal Processing Institute at SDSU, San Diego, CA, as a visiting research fellow. Currently, he is a Full Professor and the Head of the Unit of Electrical Engineering at the newly formed Tampere University, Finland. His general research interests include radio communications, radio localization, and radio-based sensing, with particular emphasis on 5G and 6G mobile radio networks.